STONY BROOK UNIVERSITY

CEAS Technical Report 832

Divisible Load Scheduling in Clustered Wireless Sensor Networks

Kijeung Choi and Thomas G. Robertazzi

December 15, 2009

Divisible Load Scheduling in Clustered Wireless Sensor Networks

Kijeung Choi and Thomas G. Robertazzi

December 15, 2009

Department of Electrical and Computer Engineering
Stony Brook University
Stony Brook, NY, 11794
Email: {kchoi, tom}@ece.sunysb.edu

Abstract

Optimal data scheduling strategies in a clustered hierarchical wireless sensor network are investigated. Data aggregation scheme in clusterheads are considered. Information utility, a newly introduced parameter is used for the situation of sensing data with a certain ratio of data accuracy in the context of the measurement data. A mathematical scheduling technique for multi-cluster wireless sensor network topology is examined by collapsing single clusters into equivalent intelligent sensor nodes which form a flat tree network. Using the optimal solution for the amount of data obtained by divisible load theory, an analysis of the energy dissipation is carried out with speed parameters and information utility constant. Aerospace based wireless sensor networks have application including tracking, environmental monitoring, and avionics sensing and control.

Chapter 1

Introduction

In recent years, wireless sensor networks (WSNs) have been a dynamically growing and promising research area due to the great technological progress in the field of wireless communication protocols [1]. Miniaturized low power wireless sensor devices have been used in various potential applications such as for military / aerospace communications and tracking, environmental monitoring, and avionics controls, etc. These sensors, capable of sensing, processing (aggregating) data, and short range communication, form WSNs to report aggregated data across platforms on or above geographically diverse terrain with highly constrained resources.

The applications of sensors in aerospace applications are quite diverse such as pressure sensors, speed sensors, surface temperature sensors, proximity sensors and remote sensors, etc. Such sensor applications operate as a network with various sized independent sensor clusters feeding information to a sink. In sensing, it is inevitable to obtain redundant information such as overlapped data and noninformative data. Considering that an extremely fast response is generally required in aerospace applications, data aggregation in the clusterhead is highly desired for reducing unnecessary load under data communication and computation.

As a WSN configuration, a WSN can be *flat* or *hierarchical* [2]. In flat networks, every sensor has the same functionality. On the other hand, in hierarchical networks, there are two types of sensor: a cluster head and a non clusterhead sensor. The clusterhead is usually an optimally elected high energy sensor which has a larger role than other sensors [3]. Clusterheads play an important role in data aggregation (data fusion) [4].

As compared with earlier work when most deployed WSNs involved relatively small numbers of sensors, nowadays, WSNs are considered as large scale ran-

domly and densely distributed sensor networks, which do not need infrastructure. Due to the nature of distributed sensing, it is expected that Divisible Load Theory (DLT) could play an important role in providing an optimal solution for load distribution under WSN environments, especially those having various energy and computational constraints. Considerable research has been focus at DLT since 1988 [7, 8, 9, 10, 11, 12, 13, 14, 15, 16, 17, 18, 19, 20, 21, 22, 23, 24]. A key feature of this divisible load scheduling theory (DLT) is that it uses a linear mathematical model. This is a powerful concept for the performance analysis of networks of processors and links. In divisible load scheduling theory it is assumed that computation and communication loads can be arbitrarily partitioned into small fractions and distributed among processors and links in the network. There are no precedence relations among the loads. A recursive deterministic mathematical formulation is used.

Recently, studies about DLT based WSN scheduling for data reporting have been published [20, 21]. To our knowledge, the naive data collected by clusterhead from non-clusterhead nodes would not contain the most critical information. For this reason, we introduce a parameter, the information utility constant, showing the accuracy of the collected data from each sensor. From a mathematical point of view, the information utility constant is required to be a deterministic a priori known variable to be applied to DLT. This is feasible by using a technique of information accuracy estimation [6] with a crucial assumption that the clusterhead has an accurate knowledge of position of each sensor nodes in the cluster [5]. By eliminating the noninformative part of the collected data, unexpected communication and processing delays can be reduced. We assume that the aggregation scheme perfectly filters the most critical information so that a clusterhead reports the most critical information to the sink.

The remainder of this paper is organized as follows. Chapter 2 present the types of notations and analytic background. In chapter 3, four different single cluster WSN scheduling models are analyzed. Muti-cluster WSN scheduling scheme is examined in chapter 4. Chapter 5 presents performance evaluation curves. Chapter 6 is a conclusion and a discussion of open questions.

Chapter 2

Problem Formulation and Preliminary Remarks

In a hierarchical WSN, the network sensor nodes are partitioned into groups called clusters. A cluster is composed of a single *clusterhead* and sensor nodes (non-clusterhead nodes) in the lowest tier as shown in Fig. 2.1(a). Once a cluster is created, the clusterhead distributes measurement instructions to the sensor nodes deployed in its cluster region. Sensory data from each sensor node is reported to the clusterhead in the higher tier for data aggregation (data fusion). The idea of data aggregation is to gather the data reported from different sensor nodes while eliminating redundancy, minimizing the amount of reporting, and thus achieving energy efficiency [4]. The aggregated data is then transmitted to the high power sink (Base Station, BS) in the highest tier. The BS usually routes the received data via wired infrastructure connected to Internet-based user applications. However, the networking via the wired interface between the BS and end-user is beyond our scope. Thus, the structure of WSN topology discussed in this paper is a three tier hierarchical WSN.

In this paper, we ignore the capability of sensing of clusterheads in spite of the fact that a clusterhead is an optimally elected sensor in the cluster region as we mentioned before. Here, there is no direct communication between sensor nodes. In other words, sensor nodes can communicates only through the clusterhead. We will not discuss the case of communication between node sensors in this paper. However, this important point gives us an idea that the network topology of a cluster can be considered as a centralized single level tree (star) network as shown in Fig. 2.1(a). The communication delay caused by the initial deployment of the measurement instruction from the sink to the clusterhead is ignored in the

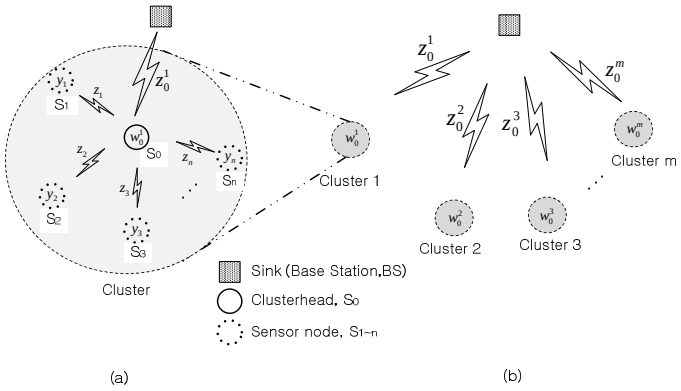

Figure 2.1: Three tier hierarchical wireless sensor network topology.

analysis in this paper. This is the based on the assumption that channel speed between sink and clusterhead is much faster than channel speed in the cluster and also the amount of instruction data is much smaller compared to the amount of sensory data. In this paper, we ignore possible limitations subject to various sources of unreliability and other issues related with wireless data transmission such as channel noise and interference during wireless transmission, etc.

The following notation is used in this paper.

t : Constant time for the instruction assignment from clusterhead to sensor nodes.

α_{si} : The sensory load fraction that the i^{th} sensor node collects.

α_{ti} : The informative load fraction (which is the critical data in response to the instruction) in the sensory load fraction that the i^{th} sensor node collects.

ρ_i : The information utility constant of the i^{th} sensor node: $\rho_i = \frac{\alpha_{ti}}{\alpha_{si}}$, the transmit to sense ratio. The parameter shows the accuracy of the data provided by the i^{th} sensor.

y_i : The inverse sensing speed of the i^{th} sensor node.

z_i : The inverse communication (reporting) speed of the link (channel) between the i^{th} sensor node and the clusterhead. We use index 0 for the clusterhead.

w_0 : The inverse computing speed of the clusterhead.

$T_{so(cp,cm)}$: Sensing operation intensity (Computing intensity, Communication intensity) constant. The entire load can be sensed (processed, transmitted) over the i^{th} channel in time $y_i T_{so}$ ($w_0 T_{cp}$, $z_i T_{cm}$).

w_0^k : The inverse computing (data aggregation) speed of the k^{th} clusterhead (where $k = 1, 2, \ldots, n$). Note that we use w_0 for analyzing a single cluster topology in this paper.

z_0^k : The inverse communication (reporting) speed of the link (channel) between the k^{th} clusterhead and a sink. Note that we use z_0 for analyzing a single cluster topology in this paper.
T_i : The total time that elapses between the beginning of the process at $t = 0$ and the time when the i^{th} sensor node completes the report of its own sensing data to the clusterhead (where $i = 1, 2, \ldots, n$). We use index 0 for the clusterhead.
$T_{r,n}$: The round time. Time at which the clusterhead for n sensors finishes transmitting the aggregated data to the sink (=T_0).
$T_{r,1}$: The round time. Time at which the clusterhead in a cluster with a single sensor node finishes transmitting the aggregated data to the sink.
We will distinguish in the following sections between different channel characteristic ($Single$, $Multi$) and whether either is equipped with front-end processor ($Simultaneous$ reporting) or not ($Sequential$ reporting). There are thus four scheduling scenarios with these two sets of possible features.

Chapter 3

Single Cluster based hierarchical WSN scheduling

3.1 Single Channel with no front-end processor, SCnP

Consider a single channel cluster composed of single clusterhead and n sensor nodes in the wireless network (star topology). This is a simple network scenario where the n sensor nodes $S_1, S_2, \ldots, S_n$ can report their own sensory data directly to the clusterhead, S_0 via a single channel. Conversely, the clusterhead can assign measurement instructions directly to the n sensor nodes via a single channel. Since all of the data flows through the single channel, sensing instruction assignment and reporting are performed sequentially as shown in Fig. 3.1. In this section, the clusterhead and sensor nodes are not equipped with front-end processors for communication off-loading. That is, nodes can either communicate (report) or sense but not do both at the same time (i.e., staggered start). In the same manner, the data aggregation is performed only after the last report from the sensors terminates, and the data aggregation and its reporting to the sink are also performed sequentially. Each sensor node has a capability to start sensing as soon as the sensor receives its sensing instructions from the sink node. The placement of nodes $S_0, S_1, S_2, \ldots$,and S_n is unconstrained. Initially, we consider that the position of the clusterhead is optimized.
From the timing diagram (Fig. 3.1), one can set up the following corresponding

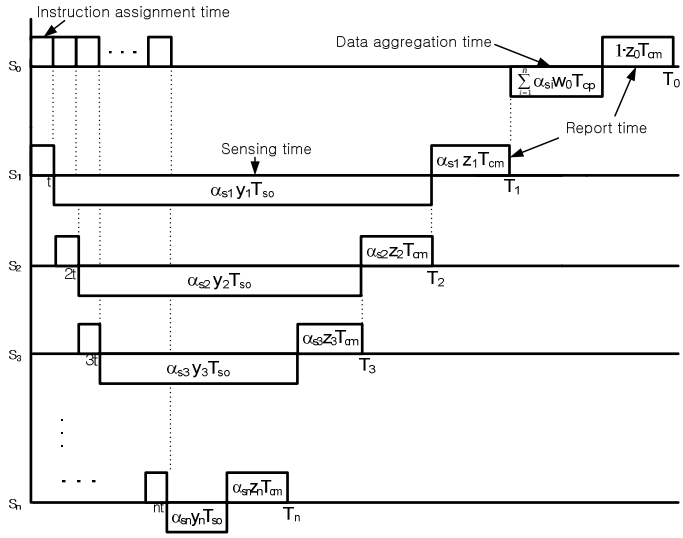

Figure 3.1: Timing diagram for single channel hierarchical wireless sensor network with no front-end processors.

recursive load distribution equations

$$\alpha_{si} y_i T_{so} = t + \alpha_{si+1}(y_{i+1} T_{so} + z_{i+1} T_{cm}) \qquad i = 1, 2, \ldots, n-1 \tag{3.1}$$

Rewriting the above set of equations as

$$\alpha_{si+1} = f_i \alpha_{si} - g_i \qquad i = 1, 2, \ldots, n-1 \tag{3.2}$$

where

$$f_i = \frac{y_i T_{so}}{y_{i+1} T_{so} + z_{i+1} T_{cm}}, \quad g_i = \frac{t}{y_{i+1} T_{so} + z_{i+1} T_{cm}} \qquad i = 1, 2, \ldots, n-1 \tag{3.3}$$

These equations can be solved as follows:

$$\begin{aligned}
\alpha_{s2} &= f_1\alpha_{s1} - g_1 \\
\alpha_{s3} &= f_2\alpha_{s2} - g_2 = f_1f_2\alpha_{s1} - g_1f_2 - g_2 \\
\alpha_{s4} &= f_3\alpha_{s3} - g_3 = f_1f_2f_3\alpha_{s1} - g_1f_2f_3 - g_2f_3 - g_3 \\
&\vdots \\
\alpha_{sn} &= f_{n-1}\alpha_{sn-1} - g_{n-1} \\
&= f_1f_2\ldots f_{n-1}\alpha_{s1} - g_1f_2f_3\ldots f_{n-1} - g_2f_3f_4\ldots f_{n-1} \\
&\quad - \ldots - g_{n-2}f_{n-1} - g_{n-1}
\end{aligned} \tag{3.4}$$

alternatively,

$$\alpha_{si} = \alpha_{s1}\prod_{k=1}^{i-1} f_k - \sum_{k=1}^{i-1}\frac{g_k}{f_k}\prod_{l=k}^{i-1} f_l \qquad i = 2, 3, \ldots, n \tag{3.5}$$

or by definition of the information utility constant

$$\begin{aligned}
\alpha_{ti} &= \rho_i\alpha_{si} \\
&= \alpha_{s1}\rho_i\prod_{k=1}^{i-1} f_k - \rho_i\sum_{k=1}^{i-1}\frac{g_k}{f_k}\prod_{l=k}^{i-1} f_l \qquad i = 2, 3, \ldots, n
\end{aligned} \tag{3.6}$$

Since the fractions of total informative data, α_ts should sum to one (normalization),

$$\begin{aligned}
1 &= \sum_{i=1}^{n}\alpha_{ti} = \sum_{i=1}^{n}\rho_i\alpha_{si} \\
&= \alpha_{s1}\left(\rho_1 + \sum_{i=2}^{n}\rho_i\prod_{k=1}^{i-1} f_k\right) - \sum_{i=2}^{n}\rho_i\sum_{k=1}^{i-1}\frac{g_k}{f_k}\prod_{l=k}^{i-1} f_l
\end{aligned} \tag{3.7}$$

Therefore,

$$\alpha_{t1} = \rho_1\alpha_{s1} = \rho_1\frac{1 + C_1}{\rho_1 + C_2} \tag{3.8}$$

where

$$C_1 = \sum_{i=2}^{n}\rho_i\left(\sum_{k=1}^{i-1}\frac{g_k}{f_k}\prod_{l=k}^{i-1} f_l\right),\ C_2 = \sum_{i=2}^{n}\rho_i\prod_{k=1}^{i-1} f_k \tag{3.9}$$

From the (3.6) and (3.8), the optimal values of α_t's, which is certain fraction of informative data collected during measurement time can be obtained. Here, we say that the network completes a *round* when the clusterhead finishes reporting the aggregated data to the sink node. Referring the Fig. 3.1, the minimum round time of the network can be achieved using (3.5) as follows

$$\begin{aligned} T_{r,n} &= T_0 \\ &= T_1 + \sum_{i=1}^{n} \alpha_{si} w_0 T_{cp} + 1 \cdot z_0 T_{cm} \\ &= t + \alpha_{s1}(y_1 T_{so} + z_1 T_{cm}) + \\ &\left\{ \alpha_{s1} \left(1 + \sum_{i=2}^{n} \prod_{k=1}^{i-1} f_k \right) - \sum_{i=2}^{n} \sum_{k=1}^{i-1} \frac{g_k}{f_k} \prod_{l=k}^{i-1} f_l \right\} w_0 T_{cp} + \\ &z_0 T_{cm} \end{aligned} \tag{3.10}$$

From (3.8), $T_{r,n}$ can be rewritten as follow

$$T_{r,n} = t + \frac{1 + C_1}{\rho_1 + C_2}(y_1 T_{so} + z_1 T_{cm}) + C_3 w_0 T_{cp} + z_0 T_{cm} \tag{3.11}$$

Here,

$$C_3 = \frac{(1 + C_1)(1 + C_2')}{\rho_1 + C_2} - C_1' \tag{3.12}$$

where,

$$C_1' = \sum_{i=2}^{n} \sum_{k=1}^{i-1} \frac{g_k}{f_k} \prod_{l=k}^{i-1} f_l,\ C_2' = \sum_{i=2}^{n} \prod_{k=1}^{i-1} f_k \tag{3.13}$$

As a special case, consider the situation of a homogeneous cluster where all sensor nodes have same inverse sensing speed and inverse communication speed (i.e., $y_i = y$, $z_i = z$ for $i = 1, 2, \ldots, n$). Note here that the inverse communication speed of the clusterhead, z_0 can be different. Consequently,

$$f = \frac{y T_{so}}{y T_{so} + z T_{cm}},\ g = \frac{t}{y T_{so} + z T_{cm}} \tag{3.14}$$

Here, $0 < f < 1$. Then, the (3.9) can be modified as

$$C_1 = \frac{g}{1 - f} \sum_{i=2}^{n} \rho_i (1 - f^{i-1}),\ C_2 = \sum_{i=2}^{n} \rho_i f^{i-1} \tag{3.15}$$

Hence, under the homogeneous condition, $T_{r,n}$ can be obtained as follow

$$T_{r,n} = t + \frac{1 + C_1}{\rho_1 + C_2}(yT_{so} + zT_{cm}) + C_3 w_0 T_{cp} + z_0 T_{cm} \tag{3.16}$$

Here, C_3 is identical form with (3.12), where

$$\begin{aligned} C_1' &= \frac{g}{f}\sum_{i=2}^{n}\left(\sum_{k=1}^{i-1}\prod_{l=k}^{i-1} f\right) = \frac{g}{f}\sum_{i=2}^{n}\sum_{k=1}^{i-1} f^{i-1-k} \\ &= \frac{g}{1-f}\left\{(n-1) - \frac{f - f^n}{1-f}\right\} \\ C_2' &= \sum_{i=2}^{n}\prod_{k=1}^{i-1} f = \sum_{i=1}^{n-1} f^i = \left(\frac{f - f^n}{1-f}\right) \end{aligned} \tag{3.17}$$

For the further simplification, here we add another special condition, $\rho_i = \rho$ for $i = 1, 2, \ldots, n$, the homogeneous information utility constant. Since $C_1 = \rho C_1'$, $C_2 = \rho C_2'$ (i.e., $C_3 = \frac{1}{\rho}$ from (3.12)) under the special case of the homogeneous (fully homogeneous, i.e. $y_i = y$, $z_i = z$, $\rho_s = \rho$ and $\rho_i = \rho$ for $i = 1, 2, \ldots, n$) condition one can solve for α_{s1} as

$$\alpha_{s1} = \frac{\frac{1}{\rho} + C_1'}{1 + C_2'} \tag{3.18}$$

Hence, $T_{r,n}$ can be obtained as follow

$$T_{r,n} = t + \frac{\frac{1}{\rho} + C_1'}{1 + C_2'} yT_{so} + \frac{\frac{1}{\rho} + C_1'}{1 + C_2'} zT_{cm} + \frac{1}{\rho} w_0 T_{cp} + z_0 T_{cm} \tag{3.19}$$

From the above equation, under the fully homogeneous condition, we can readily see the minimum round time can be achieved when information utility constant equals to unity which is an ideal case. This makes intuitive sense as no redundant data is generated, time delays for sensing, reporting, and data aggregation can be reduced.

Since the minimum round time on a single sensor node under the homogeneous condition is

$$T_{r,1} = t + \frac{1}{\rho} yT_{so} + \frac{1}{\rho} zT_{cm} + \frac{1}{\rho} w_0 T_{cp} + z_0 T_{cm} \tag{3.20}$$

the speedup is then

$$Speedup = \frac{t + \frac{1}{\rho} yT_{so} + \frac{1}{\rho} zT_{cm} + \frac{1}{\rho} w_0 T_{cp} + z_0 T_{cm}}{t + \frac{\frac{1}{\rho}+C_1'}{1+C_2'} yT_{so} + \frac{\frac{1}{\rho}+C_1'}{1+C_2'} zT_{cm} + \frac{1}{\rho} w_0 T_{cp} + z_0 T_{cm}} \tag{3.21}$$

Under the fully homogeneous condition, the condition for a feasible instruction assignment time, t can be described. From the Fig. 2, under the case of the sequential distribution under the single channel scenario, it can be possible some sensors cannot be assigned the instruction under the certain condition that the instruction assignment time is large. Referring to (3.5), the upper bound of a feasible instruction assignment time constant can be obtained according to the intuitive condition as

$$\begin{aligned} & 0 < \alpha_{si} < 1 \qquad i = 2, 3, \ldots, n \\ & < \alpha_{s1} f^{i-1} - \frac{g}{f}\left(\frac{f - f^{i-1}}{1-f}\right) < 1 \\ & < \frac{\frac{1}{\rho} + C_1'}{1 + C_2'} f^{i-1} - \frac{g}{f}\left(\frac{f - f^{i-1}}{1-f}\right) < 1 \\ & < \frac{\frac{1}{\rho}}{1 + C_2'} f^{i-1} + \left\{ \frac{C_1''}{1 + C_2'} f^{i-1} + \frac{1}{yT_{so}}\left(\frac{f - f^{i-1}}{1-f}\right) \right\} t < 1 \end{aligned} \tag{3.22}$$

where, $C_1'' = C_1'/t$ (refer to (3.17)).
Thus, we have

$$0 < \eta_i + \gamma_i t < 1 \qquad i = 2, 3, \ldots, n \tag{3.23}$$

where,

$$\begin{aligned} \eta_i &= \frac{\frac{1}{\rho}}{1 + C_2'} f^{i-1} \\ \gamma_i &= \frac{C_1''}{1 + C_2'} f^{i-1} + \frac{1}{yT_{so}}\left(\frac{f - f^{i-1}}{1-f}\right) \end{aligned} \tag{3.24}$$

Since, $\eta_i > 0$, if $\gamma_i < 0$, the (3.23) can be rewritten as follows

$$0 \le t < \frac{\eta_k}{\gamma_k} \tag{3.25}$$

Here, k is the index of the sensor node number where $\gamma_i < 0$. If $\gamma_i > 0$, the (3.23) can be rewritten as follows

$$0 \leq t < \frac{1-\eta_l}{\gamma_l} \tag{3.26}$$

Here, l is the index of the sensor node number where $\gamma_i > 0$. From the (3.25) and (3.26), the condition for the feasible instruction assignment time, t_{feas} can be written as

$$0 \leq t_{feas} < min(\frac{\eta_k}{\gamma_k}, \frac{1-\eta_l}{\gamma_l}) \tag{3.27}$$

Here, if one let $n \to \infty$, we can superficially recognize that $T_{r,n} \to \infty$, which is not reasonable since the factor, $C_1^{'}$ is a the first order function of n (see (3.17)). However, as referring the bound for feasible t (see (3.25) and (3.26)), we would also see $t \to 0$ (i.e., $C_1^{''} \to \infty$ or $\gamma_i \to \infty$) as one is adding more sensor nodes in the cluster.
Hence, using the fact $C_1^{'} \to 0$ and $C_2^{'} \to \frac{yT_{so}}{zT_{cm}}$, one can obtain the asymptotic minimum round time, $T_{r,\infty}$ as

$$\begin{aligned} T_{r,\infty} &= \frac{\sigma}{\rho(\sigma+1)} yT_{so} + \frac{\sigma}{\rho(\sigma+1)} zT_{cm} + \frac{1}{\rho} w_0 T_{cp} + z_0 T_{cm} \\ &= \frac{1}{\rho} zT_{cm} + \frac{1}{\rho} w_0 T_{cp} + z_0 T_{cm} \end{aligned} \tag{3.28}$$

where $\sigma = \frac{zT_{cm}}{yT_{so}}$
From (3.21), we can obtain asymptotic speedup as follows

$$Speedup_{n\to\infty} = 1 + \frac{yT_{so}}{zT_{cm} + w_0 T_{cp} + \rho z_0 T_{cm}} \tag{3.29}$$

3.2 Multi Channel with no front-end processor, MCnP

The network model that is discussed in this subsection is similar to that discussed in the previous one except for the fact that the communication between the clusterhead and sensor nodes takes place under multiple independent channels. Therefore, multiple access to the clusterhead from the sensor nodes can take place at the

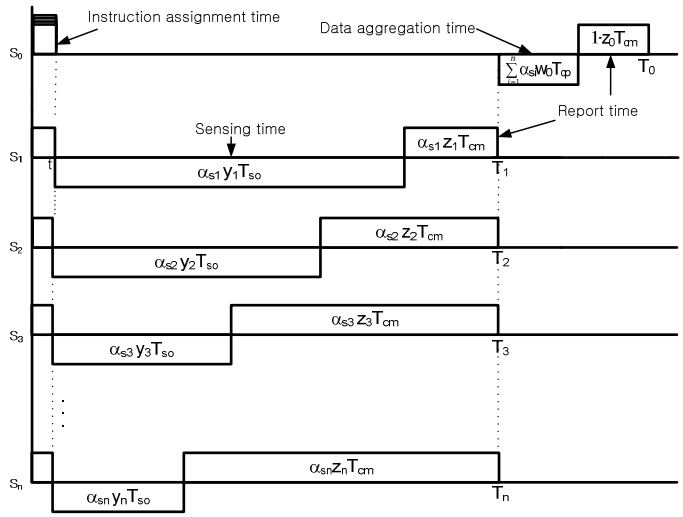

Figure 3.2: Timing diagram for multi channel hierarchical wireless sensor network with no front-end processors.

same time. Conversely, concurrent instruction assignment is feasible as described in Fig. 3.2. As a reminder, the single channel case gives rises to considerable idle time for almost all of the sensor nodes due to the sequential communication (instruction assignment and reporting) involved in communicating data from each sensor node to the clusterhead. On the other hand, communication delay is reduced through simultaneous instruction assignment and mainly simultaneous reporting termination over all sensor nodes through multiple channels. It has been known on a intuitive basis that network elements should be kept constantly busy for good performance [16, 17]. Thus it can be expected that multi channel communication contributes to better performance than the single channel scenario in that each sensor finish the reporting simultaneously.
The timing diagram of the network is plotted in Fig. 3.2. The fundamental recursive equation of the network can be formulated as follows

$$t + \alpha_{si}(y_i T_{so} + z_i T_{cm}) = t + \alpha_{si+1}(y_{i+1} T_{so} + z_{i+1} T_{cm}) \qquad i = 1, 2, \ldots, n-1 \tag{3.30}$$

Rewriting the above set of equations as

$$\alpha_{si+1} = f_i \alpha_{si} \qquad i = 1, 2, \ldots, n-1 \tag{3.31}$$

where

$$f_i = \frac{y_i T_{so} + z_i T_{cm}}{y_{i+1} T_{so} + z_{i+1} T_{cm}} \qquad i = 1, 2, \ldots, n-1 \tag{3.32}$$

These equations can be solved as follows

$$\alpha_{si} = \alpha_{s1} \prod_{k=1}^{i-1} f_k \qquad i = 2, 3, \ldots, n \tag{3.33}$$

Alternatively, by definition of information the utility constant

$$\alpha_{ti} = \rho_i \alpha_{si} = \alpha_{s1} \rho_i \prod_{k=1}^{i-1} f_k \qquad i = 2, 3, \ldots, n \tag{3.34}$$

As mentioned earlier, the fractions of the total informative data should sum to one

$$1 = \sum_{i=1}^{n} \alpha_{ti} = \sum_{i=1}^{n} \rho_i \alpha_{si} = \alpha_{s1} \left(\rho_1 + \sum_{i=2}^{n} \rho_i \prod_{k=1}^{i-1} f_k \right) \tag{3.35}$$

Therefore,

$$\alpha_{t1} = \rho_1 \alpha_{s1} = \rho_1 \frac{1}{\rho_1 + C_1} \tag{3.36}$$

where

$$C_1 = \sum_{i=2}^{n} \rho_i \prod_{k=1}^{i-1} f_k \tag{3.37}$$

From (3.34) and (3.36), the optimal values of α_t's, which is the fraction of informative data collected during measurement time can be obtained.
Knowing the optimal value of α_{s1}, the minimum round time can be calculated as

$$\begin{aligned} T_{r,n} &= T_0 \\ &= T_1 + \sum_{i=1}^{n} \alpha_{si} w_0 T_{cp} + 1 \cdot z_0 T_{cm} \\ &= t + \alpha_{s1}(y_1 T_{so} + z_1 T_{cm}) + \\ &\alpha_{s1} \left(1 + \sum_{i=2}^{n} \prod_{k=1}^{i-1} f_k \right) w_0 T_{cp} + z_0 T_{cm} \end{aligned} \tag{3.38}$$

From $\alpha_{s1} = \frac{1}{\rho_1 + C_1}$ (see (3.36)), $T_{r,n}$ can be rewritten as follow

$$T_{r,n} = t + \frac{1}{\rho_1 + C_1}(y_1 T_{so} + z_1 T_{cm}) + C_3 w_0 T_{cp} + z_0 T_{cm} \tag{3.39}$$

where

$$C_1^{'} = \sum_{i=2}^{n} \prod_{k=1}^{i-1} f_k,\ C_3 = \frac{1 + C_1^{'}}{\rho_1 + C_1} \tag{3.40}$$

As a special case, consider the situation of a homogeneous cluster where all sensor nodes have same inverse sensing speed and inverse communication speed (i.e., $y_i = y$, $z_i = z$ for $i = 1, 2, \ldots, n$). Note here that the inverse communication speed of the clusterhead, z_0 can be different. Consequently, $f = 1$ (i.e., $C_1 = \sum_{i=2}^{n} \rho_i$ and $C_1^{'} = n - 1$).
In this case, one can solve for α_{s1} as

$$\alpha_{s1} = \frac{1}{\sum_{i=1}^{n} \rho_i} \tag{3.41}$$

The minimum round time is then given by

$$T_{r,n} = t + \frac{1}{\sum_{i=1}^{n} \rho_i}(y T_{so} + z T_{cm} + n w_0 T_{cp}) + z_0 T_{cm} \tag{3.42}$$

For further simplification, consider the situation of a fully homogeneous network (i.e. $y_i = y$, $z_i = z$, and $\rho_i = \rho$ for $i = 1, 2, \ldots, n$). Consequently, $f = 1$ (i.e., $C_1 = \rho(n-1)$ and $C_1^{'} = n - 1$).
In this case, one can solve for α_{s1} as

$$\alpha_{s1} = \frac{1}{\rho n} \tag{3.43}$$

Intuitively, the equal amount of informative (sensed) data (i.e., $\frac{1}{n}$) is reasonable due to the simultaneous measurement start time and reporting finish time under the fully homogeneous condition.
The minimum round time is then given by

$$T_{r,n} = t + \frac{1}{\rho n} y T_{so} + \frac{1}{\rho n} z T_{cm} + \frac{1}{\rho} w_0 T_{cp} + z_0 T_{cm} \tag{3.44}$$

From the above equation, under the fully homogeneous condition, we can also see the minimum round time can be achieved when information utility constant equals to unity which is an ideal case. This also follows intuition as no redundant data is generated, time delays for sensing, reporting, and data aggregation can be reduced.
Since the minimum round time on a single sensor node under the homogeneous condition is

$$T_{r,1} = t + \frac{1}{\rho} y T_{so} + \frac{1}{\rho} z T_{cm} + \frac{1}{\rho} w_0 T_{cp} + z_0 T_{cm} \tag{3.45}$$

the speedup is then

$$Speedup = \frac{t + \frac{1}{\rho} y T_{so} + \frac{1}{\rho} z T_{cm} + \frac{1}{\rho} w_0 T_{cp} + z_0 T_{cm}}{t + \frac{1}{\rho n} y T_{so} + \frac{1}{\rho n} z T_{cm} + \frac{1}{\rho} w_0 T_{cp} + z_0 T_{cm}} \tag{3.46}$$

The asymptotic minimum round time, $T_{r,\infty}$ can be simply written as

$$T_{r,\infty} = t + \frac{1}{\rho} w_0 T_{cp} + z_0 T_{cm} \tag{3.47}$$

The asymptotic speedup can be obtain as follows

$$Speedup_{n \to \infty} = 1 + \frac{y T_{so} + z T_{cm}}{\rho t + w_0 T_{cp} + \rho z_0 T_{cm}} \tag{3.48}$$

3.3 Single Channel with front-end processor, SCP

The network model that is discussed in this subsection is similar to that discussed in subsection 3.1 except for the fact that each of n sensor nodes and clusterhead are equipped with a front-end processor for communicating off-loading. That is, the sensor nodes can communicate (report) and sense at the same time. The clusterhead can perform the data aggregation as it gathers sensory data from each sensor node. We assume here, the data aggregation is started immediately after the first sensory data is reported as shown in Fig. 3.3. Intuitively, the reporting time lasts at least when sensing operation terminates. In this subsection, we assume that $z_i T_{cm} < y_i T_{so}$, so that reporting of sensory data at each sensor node can end with sensing operation at the same instant even though the i^{th} reporting

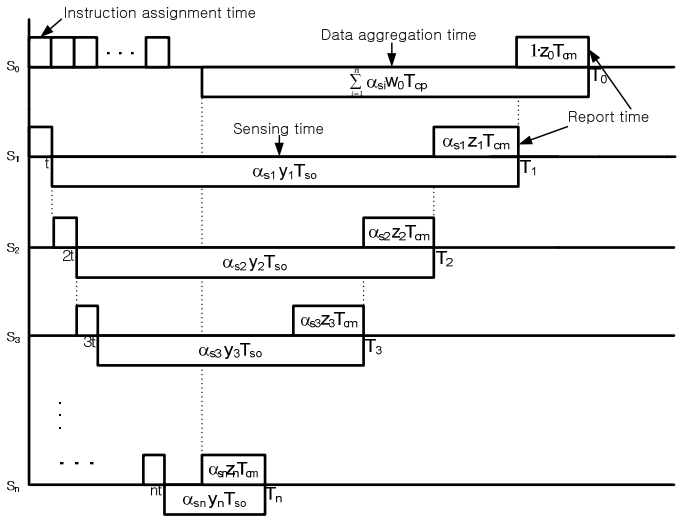

Figure 3.3: Timing diagram for single channel hierarchical wireless sensor network with front-end processors.

starts when the $(i+1)^{th}$ sensor nodes terminates its own reporting (Fig. 3.3). Surely, each report can be started only after the sensing operation is started. For the clusterhead, we can conjecture $\sum_{i=1}^{n} \alpha_{si} w_0 T_{cp} - z_0 T_{cm} \leq \sum_{i=1}^{n} \alpha_{si} z_i T_{cm}$ to meet the minimum round time. Here, we can see that the conjecture also implies $z_0 T_{cm} \leq \sum_{i=1}^{n} \alpha_{si} w_0 T_{cp}$ so that reporting to sink (BS) and data aggregation end at the same time.
According to Fig. 3.3, the fundamental recursive equation of the network can be obtained as follows:

$$\alpha_{si} y_i T_{so} = t + \alpha_{si+1} y_{i+1} T_{so} + \alpha_{si} z_i T_{cm} \qquad i = 1, 2, \ldots, n-1 \tag{3.49}$$

One can rewriting the above set of equations as

$$\alpha_{si+1} = f_i \alpha_{si} - g_i \qquad i = 1, 2, \ldots, n-1 \tag{3.50}$$

Here, the above equation has the same formation with (3.2), but

$$f_i = \frac{y_i T_{so} - z_i T_{cm}}{y_{i+1} T_{so}}, \;\; g_i = \frac{t}{y_{i+1} T_{so}} \qquad i = 1, 2, \ldots, n-1 \tag{3.51}$$

As we mentioned previously, $z_i T_{cm} < y_i T_{so}$. That is, communication speed must be faster than sensing speed. The optimal values of α_ts can be obtained using eq (3.6) and (3.8).
Referring the Fig. 3.3, the minimum round time, $T_{r,n}$ can be then obtained as follows

$$\begin{aligned} T_{r,n} = min(T_0) &= T_1 + z_0 T_{cm} \\ &= t + \alpha_{s1} y_1 T_{so} + z_0 T_{cm} \end{aligned} \tag{3.52}$$

Note that $min(T_0)$ is derived according to the condition, $\sum_{i=1}^{n} \alpha_{si} w_0 T_{cp} - z_0 T_{cm} = \sum_{i=1}^{n} \alpha_{si} z_i T_{cm}$ as we mentioned previously.
Using eq (3.8) and (3.9), $T_{r,n}$ can be rewritten as follow

$$T_{r,n} = t + \frac{1 + C_1}{\rho_1 + C_2} y_1 T_{so} + z_0 T_{cm} \tag{3.53}$$

As a special case, consider the situation of a fully homogeneous network (i.e. $y_i = y$, $z_i = z$, and $\rho_i = \rho$ for $i = 1, 2, \ldots, n$). Note here that the inverse communication speed of the clusterhead, z_0 can be different.
Consequently,

$$f = 1 - \frac{z T_{cm}}{y T_{so}},\ g = \frac{t}{y T_{so}} \tag{3.54}$$

Here, $y T_{so} > z T_{cm}$. Thus $0 < f < 1$.
Also, under the fully homogeneous condition the initial two conjectures we mentioned previously,
$\sum_{i=1}^{n} \alpha_{si} w_0 T_{cp} - z_0 T_{cm} \leq \sum_{i=1}^{n} \alpha_{si} z_i T_{cm}$ and $z_0 T_{cm} \leq \sum_{i=1}^{n} \alpha_{si} w_0 T_{cp}$, can be combined as follows

$$\rho \leq \frac{w_0 T_{cp}}{z_0 T_{cm}} \leq \rho + \frac{z T_{cm}}{z_0 T_{cm}} \tag{3.55}$$

The above inequality gives an information of the feasible range of the ratio of $\frac{w_0 T_{cp}}{z_0 T_{cm}}$ to meet the minimum round time.
Following similar procedures showed previous subsections, α_{s1} can be obtained as a identical form with (3.18).
The minimum round time is then given by

$$T_{r,n} = t + \frac{\frac{1}{\rho} + C_1'}{1 + C_2'} y T_{so} + z_0 T_{cm} \tag{3.56}$$

From the above equation, under a fully homogeneous condition, we can also see the minimum round time can be achieved when information utility constant equals to unity which is an ideal case.
Under the fully homogeneous condition, a closed form of the condition for a feasible instruction assignment time, t_{feas} can be derived as the similar manner shown in subsection 3.1.

$$0 \leq t_{feas} < min(\frac{\eta_k}{\gamma_k}, \frac{1-\eta_l}{\gamma_l}) \tag{3.57}$$

where,

$$\eta_i = \frac{\frac{1}{\rho}}{1+C_2'} f^{i-1}$$
$$\gamma_i = \frac{C_1''}{1+C_2'} f^{i-1} + \frac{1}{yT_{so} - zT_{cm}} \left(\frac{f - f^{i-1}}{1-f} \right) \tag{3.58}$$

Here, k and l are the index of the sensor node number where $\gamma_i < 0$ and $\gamma_i > 0$, respectively. From the above equation, under fully homogeneous condition, we can also see the minimum round time can be achieved when information utility constant equals to unity which is an ideal case.
Since the minimum round time on a single sensor node under the fully homogeneous condition is

$$T_{r,1} = t + \frac{1}{\rho} yT_{so} + z_0 T_{cm} \tag{3.59}$$

the speedup is then

$$Speedup = \frac{t + \frac{1}{\rho} yT_{so} + z_0 T_{cm}}{t + \frac{\frac{1}{\rho} + C_1'}{1+C_2'} yT_{so} + z_0 T_{cm}} \tag{3.60}$$

From the (3.56), using the fact, $C_1' \rightarrow 0$ (i.e., $t \rightarrow 0$) and $C_2' \rightarrow \frac{yT_{so}}{zT_{cm}} - 1$ as $n \rightarrow \infty$, the asymptotic minimum round time, $T_{r,\infty}$ can be simply written as

$$T_{r,\infty} = \frac{\sigma}{\rho} yT_{so} + z_0 T_{cm} = \frac{1}{\rho} zT_{cm} + z_0 T_{cm} \tag{3.61}$$

Here, $\sigma = \frac{zT_{cm}}{yT_{so}}$.
The asymptotic speedup can be then obtained as follows

$$Speedup_{n \rightarrow \infty} = \frac{yT_{so} + \rho z_0 T_{cm}}{zT_{cm} + \rho z_0 T_{cm}} \tag{3.62}$$

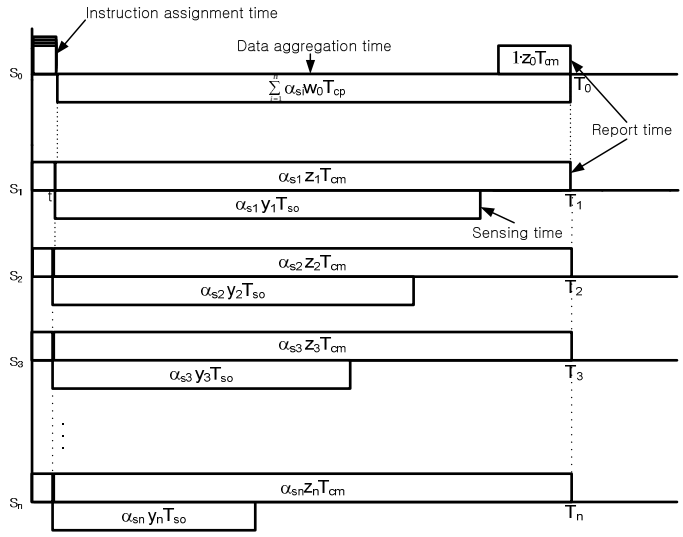

Figure 3.4: Timing diagram for multi channel hierarchical wireless sensor network with front-end processors.

3.4 Multi Channel with front-end processor, MCP

This subsection is similar to the previous one except for the fact that now the communication between sink node and sensor nodes takes place under multiple independent channels as described in subsection 3.2, so that simultaneous reporting is possible. It was shown that the simultaneous sensing operation start and simultaneous reporting termination over all sensor nodes provided through multiple independent channels contribute improved performance in subsection 3.2. Furthermore, more improvement in performance would be achieved from the simultaneous reporting termination over all nodes include the clusterhead with front-end processor. The timing diagram of the network is plotted in Fig. 3.4. We assume here that $z_i T_{cm} > y_i T_{so}$, so that the speed of sensing operation is faster than the speed of reporting. In other words, by intuitive sense, the sensing operation is required to be ceased before or exactly when the reporting terminates. For the clusterhead, we can conjecture $\sum_{i=1}^{n} \alpha_{si} w_0 T_{cp} \leq \alpha_{si} z_i T_{cm}$ to meet the minimum round time from in Fig. 3.4. Also, we can conjecture that $z_0 T_{cm} \leq \sum_{i=1}^{n} \alpha_{si} w_0 T_{cp}$ so that reporting to sink (BS) and data aggregation end at the same time. From the conjecture, we can expect that the minimum T_0 can be obtained under a certain condition, $\sum_{i=1}^{n} \alpha_{si} w_0 T_{cp} = \alpha_{si} z_i T_{cm}$.
The fundamental recursive equation which is independent of the information util-

ity, ρ can be formulated as follows:

$$\alpha_{si} z_i T_{cm} = \alpha_{si+1} z_{i+1} T_{cm} \qquad i = 1, 2, \ldots, n-1 \tag{3.63}$$

One can rewriting the above set of equations as

$$\alpha_{si+1} = f_i \alpha_{si} \qquad i = 1, 2, \ldots, n-1 \tag{3.64}$$

Here, the above equation has the same formation with (3.31), but

$$f_i = \frac{z_i T_{cm}}{z_{i+1} T_{cm}} \qquad i = 1, 2, \ldots, n-1 \tag{3.65}$$

Thus, the optimal values of α_ts can be obtained as (3.34) using the identical equation, (3.36).
Referring Fig. 3.4, the minimum round time, $T_{r,n}$ can be obtained as follows

$$T_{r,n} = min(T_0) = T_1 = t + \alpha_{s1} z_1 T_{cm} \tag{3.66}$$

Using the (3.36), $T_{r,n}$ can be rewritten as follow

$$T_{r,n} = t + \frac{1}{\rho_1 + C_1} z_1 T_{cm} \tag{3.67}$$

As a special case, consider the situation of a fully homogeneous network (i.e. $y_i = y$, $z_i = z$, and $\rho_i = \rho$ for $i = 1, 2, \ldots, n$). Note here that the inverse communication speed of the clusterhead, z_0 can be different.
Since $f = 1$ (i.e., $C_1 = \rho(n-1)$), α_{s1} can be obtained as the equal amount of sensed data shown as (3.43).
From the two initial conjecture, $\sum_{i=1}^{n} \alpha_{si} w_0 T_{cp} \leq \alpha_{si} z_i T_{cm}$ and $z_0 T_{cm} \leq \sum_{i=1}^{n} \alpha_{si} w_0 T_{cp}$, the following combined inequality can be obtained

$$\rho \leq \frac{w_0 T_{cp}}{z_0 T_{cm}} \leq \frac{z T_{cm}}{n z_0 T_{cp}} \tag{3.68}$$

The above inequality shows that as the number of sensor nodes increases the required upper bound of the ratio $\frac{w_0 T_{cp}}{z_0 T_{cm}}$ reduced. Also, from the condition, $\rho \leq \frac{z T_{cm}}{n z_0 T_{cp}}$, we can see that minimum required value of the ratio $\frac{z T_{cm}}{z_0 T_{cp}}$ is the number of sensor nodes in the cluster, n. This is expected as all the sensing operations of

sensor nodes are performed simultaneously and are also the corresponding reporting performed simultaneously, for the effective data aggregation at clusterhead, the processing speed is needed increased. The minimum round time is then given by

$$T_{r,n} = t + \frac{1}{\rho n} z T_{cm} \tag{3.69}$$

Since the minimum round time on a single sensor node under the fully homogeneous condition is

$$T_{r,1} = t + \frac{1}{\rho} z T_{cm} \tag{3.70}$$

the speedup is then

$$Speedup = \frac{t + \frac{1}{\rho} z T_{cm}}{t + \frac{1}{\rho n} z T_{cm}} \tag{3.71}$$

Note that if one consider the case that the instruction assignment time, t is negligible (i.e., $t \to 0$), speedup can be achieved as n, which is a linear function to the number of sensor nodes, that is speedup is scalable in this case.
From (3.69) and (3.71), the asymptotic minimum round time and the asymptotic speedup are given respectively as

$$T_{r,\infty} = t, \;\; Speedup_{n \to \infty} = 1 + \frac{1}{\rho t} z T_{cm} \tag{3.72}$$

Chapter 4

Multi-Cluster based hierarchical wireless sensor network scheduling

In this section, we will discuss multi-cluster three tier hierarchical WSN model based on the four scenarios we analyzed in the previous section (see Fig. 2.1(b)). The homogeneous network (i.e.,$z_0^i = z_0$, $w_0^i = w_0$, and $\rho_i = \rho$ for $i = 1, 2, \ldots, n$) is assumed for finding a closed form equation. The methodology used to analyze the multi-cluster model is to collapse a group of nodes (a clusterhead + sensor nodes) composing a cluster into a single equivalent sensor node. This methodology is similar with the one applied in several previous studies [22, 23, 24]. Based on the equivalent node element, we can collapse a cluster into a single "intelligent" sensor node. The terminology, "intelligent" is used for denoting a sensor node which performs its own data aggregation, a significant role of clusterhead. Hence, the final equivalent WSN topology would be flat, not hierarchical as shown

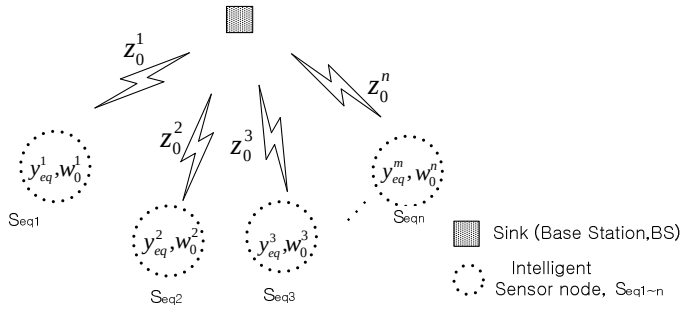

Figure 4.1: The equivalent flat wireless sensor network topology with intelligent sensor nodes

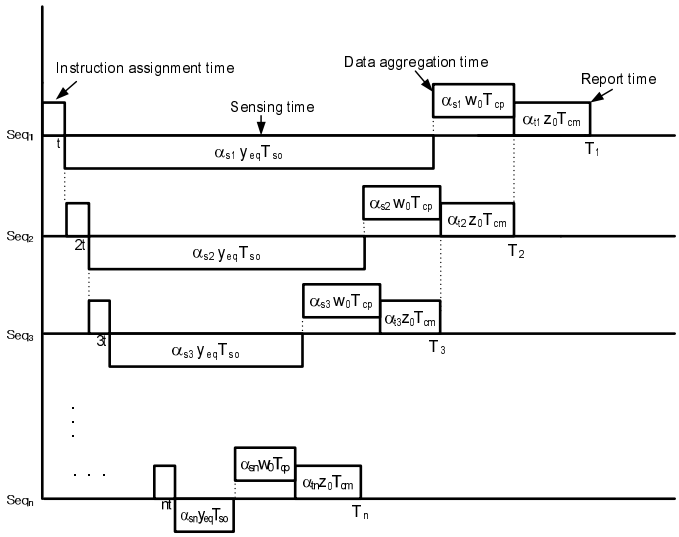

Figure 4.2: Timing diagram for single channel flat wireless sensor network with homogeneous intelligent sensors with no front-end processors.

in Fig. 4.1. As we mentioned previously, the four scenarios we will discuss in this section is similar to that analyzed in the previous one except for the fact that all sensors equally participate in the sensing operation.

4.1 Single Channel with no front-end processor

On the way of collapsing, n clusters will be replaced by n equivalent intelligent sensor nodes. Referring (3.20), the round time on a single equivalent intelligent sensor node can be written as follows

$$t + \frac{1}{\rho} y_{eq} T_{so} + \frac{1}{\rho} z T_{cm} + \frac{1}{\rho} w_0 T_{cp} + z_0 T_{cm} \tag{4.1}$$

By equating the above equation and (3.19), we can obtain y_{eq} as

$$y_{eq} = \frac{1}{T_{so}} \left\{ \frac{1 + \rho C_1'}{1 + C_2'} y T_{so} + \left(\frac{1 + \rho C_1'}{1 + C_2'} - 1 \right) z T_{cm} \right\} \tag{4.2}$$

where, C_1' and C_2' are as described in (3.17).
The timing diagram of the flat WSN with the n homogeneous intelligent sensor

nodes is illustrated in Fig. 4.2. From the timing diagram (Fig. 4.2), one can set up the following corresponding recursive load distribution equations

$$\begin{aligned}
&\alpha_{si}(y_{eq}T_{so} + w_0T_{cp}) = \\
&t + \alpha_{si+1}(y_{eq}T_{so} + w_0T_{cp}) + \alpha_{ti+1}z_0T_{cm} \\
&\qquad i = 1, 2, \ldots, n-1
\end{aligned} \tag{4.3}$$

The above set of equations can be further expressed using the information utility constant, ρ as

$$\begin{aligned}
&\alpha_{si}(y_{eq}T_{so} + w_0T_{cp}) = \\
&t + \alpha_{si+1}(y_{eq}T_{so} + w_0T_{cp}) + \rho\alpha_{si+1}z_0T_{cm} \\
&= t + \alpha_{si+1}(y_{eq}T_{so} + w_0T_{cp} + \rho z_0T_{cm}) \\
&\qquad i = 1, 2, \ldots, n-1
\end{aligned} \tag{4.4}$$

Rewriting the above set of equations as

$$\alpha_{si+1} = f\alpha_{si} - g \qquad i = 1, 2, \ldots, n-1 \tag{4.5}$$

where

$$\begin{aligned}
f &= \frac{y_{eq}T_{so} + w_0T_{cp}}{y_{eq}T_{so} + w_0T_{cp} + \rho z_0T_{cm}} \\
g &= \frac{t}{y_{eq}T_{so} + w_0T_{cp} + \rho z_0T_{cm}}
\end{aligned} \tag{4.6}$$

From the derivational similarity with subsection 3.1, we can solve for α_{s1} as (3.18). Hence, the minimum round time using n homogeneous intelligent sensor nodes, $T_{r,n}$ can be achieved as follows

$$\begin{aligned}
T_{r,n} &= T_1 \\
&= t + \alpha_{s1}(y_{eq}T_{so} + w_0T_{cp} + \rho z_0T_{cm}) \\
&= t + \frac{\frac{1}{\rho} + C_1'}{1 + C_2'}(y_{eq}T_{so} + w_0T_{cp} + \rho z_0T_{cm})
\end{aligned} \tag{4.7}$$

Since the minimum round time on a single intelligent sensor node is

$$T_{r,1} = t + \frac{1}{\rho}(y_{eq}T_{so} + w_0T_{cp} + \rho z_0T_{cm}) \tag{4.8}$$

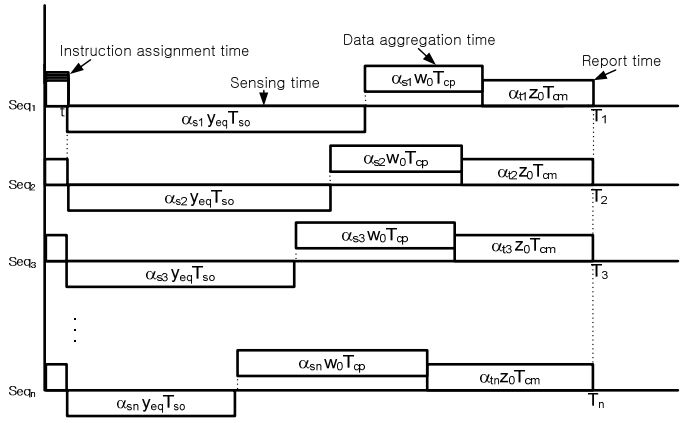

Figure 4.3: Timing diagram for multi channel flat wireless sensor network with homogeneous intelligent sensors with no front-end processor.

the speedup is then

$$Speedup = \frac{T_{r,1}}{T_{r,n}} = \frac{t + \frac{1}{\rho}(y_{eq}T_{so} + w_0T_{cp} + \rho z_0T_{cm})}{t + \frac{\frac{1}{\rho}+C_1'}{1+C_2'}(y_{eq}T_{so} + w_0T_{cp} + \rho z_0T_{cm})} \tag{4.9}$$

4.2 Multi Channel with no front-end processor

On the way of collapsing, n clusters will be replaced by n equivalent intelligent sensor nodes as we showed in the previous subsection. Referring (3.45), the round time on a single equivalent intelligent sensor node can be written as follows

$$t + \frac{1}{\rho}y_{eq}T_{so} + \frac{1}{\rho}zT_{cm} + \frac{1}{\rho}w_0T_{cp} + z_0T_{cm} \tag{4.10}$$

By equating the above equation and (3.44), we can obtain y_{eq} as

$$y_{eq} = \frac{1}{T_{so}}\left\{\frac{1}{n}yT_{so} + \left(\frac{1}{n} - 1\right)zT_{cm}\right\} \tag{4.11}$$

The timing diagram of the flat WSN with the n homogeneous intelligent sensor nodes is illustrated in Fig. 4.3. From the timing diagram (Fig. 4.3), one can set up

the following corresponding recursive load distribution equations

$$\begin{aligned} t + \alpha_{si}(y_{eq}T_{so} + w_0T_{cp}) + \alpha_{ti}z_0T_{cm} = \\ t + \alpha_{si+1}(y_{eq}T_{so} + w_0T_{cp}) + \alpha_{ti+1}z_0T_{cm} \\ i = 1, 2, \ldots, n-1 \end{aligned} \tag{4.12}$$

The above set of equations can be further expressed using the information utility constant, ρ as

$$\begin{aligned} t + \alpha_{si}(y_{eq}T_{so} + w_0T_{cp} + \rho z_0T_{cm}) = \\ t + \alpha_{si+1}(y_{eq}T_{so} + w_0T_{cp} + \rho z_0T_{cm}) \\ i = 1, 2, \ldots, n-1 \end{aligned} \tag{4.13}$$

Rewriting the above set of equations simply as

$$\alpha_{si+1} = \alpha_{si} \qquad i = 1, 2, \ldots, n-1 \tag{4.14}$$

From the intuitive similarity with $III - B$, we can solve for α_{s1} as (3.43).
Hence, the minimum round time using n homogeneous intelligent sensor nodes, $T_{r,n}$ can be achieved as follows

$$\begin{aligned} T_{r,n} &= T_1 \\ &= t + \alpha_{s1}(y_{eq}T_{so} + w_0T_{cp} + \rho z_0T_{cm}) \\ &= t + \frac{1}{\rho n}(y_{eq}T_{so} + w_0T_{cp} + \rho z_0T_{cm}) \end{aligned} \tag{4.15}$$

Since the minimum round time on a single intelligent sensor node is

$$T_{r,1} = t + \frac{1}{\rho}(y_{eq}T_{so} + w_0T_{cp} + \rho z_0T_{cm}) \tag{4.16}$$

the speedup is then

$$Speedup = \frac{T_{r,1}}{T_{r,n}} = \frac{t + \frac{1}{\rho}(y_{eq}T_{so} + w_0T_{cp} + \rho z_0T_{cm})}{t + \frac{1}{\rho n}(y_{eq}T_{so} + w_0T_{cp} + \rho z_0T_{cm})} \tag{4.17}$$

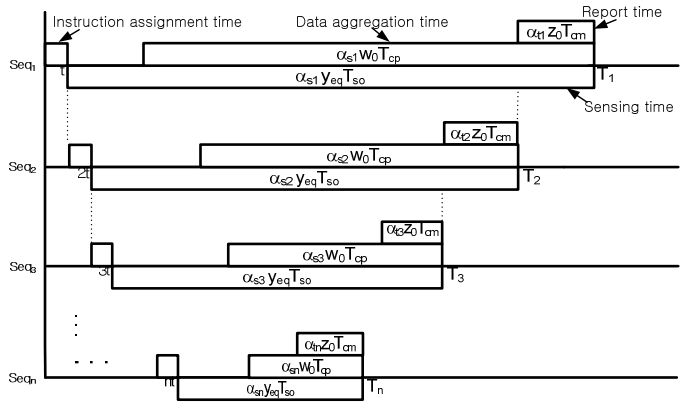

Figure 4.4: Timing diagram for single channel flat wireless sensor network with homogeneous intelligent sensors with front-end processor.

4.3 Single Channel with front-end processor

By following a similar step of collapsing showed in the previous subsections, referring (3.59), the round time on a single equivalent intelligent sensor node can be written as follows

$$t + \frac{1}{\rho} y_{eq} T_{so} + z_0 T_{cm} \tag{4.18}$$

By equating the above equation and (3.56), we can obtain y_{eq} as

$$y_{eq} = \frac{1}{T_{so}} \left(\frac{1 + \rho C_1'}{1 + C_2'} \right) y T_{so} \tag{4.19}$$

The timing diagram of the flat WSN with the n homogeneous intelligent sensor nodes is illustrated in Fig. 4.4. Here, we assume that $z_0 T_{cm} < w_0 Tcp$ so that reporting of sensory data at each sensor node can end with own data aggregation at the same instant even though the i^{th} reporting starts when the $(i+1)^{th}$ equivalent intelligent sensor nodes terminates its own reporting (Fig. 4.4). From the timing diagram (Fig. 4.4), one can set up the following corresponding recursive load distribution equations

$$\begin{aligned} \alpha_{si} y_{eq} T_{so} &= t + \alpha_{si+1} y_{eq} T_{so} + \alpha_{ti} z_0 T_{cm} \\ & \qquad i = 1, 2, \ldots, n-1 \end{aligned} \tag{4.20}$$

The above set of equations can be further expressed using the information utility constant, ρ as

$$\begin{aligned} \alpha_{si}(y_{eq}T_{so} - \rho z_0 T_{cm}) &= t + \alpha_{si+1} y_{eq} T_{so} \\ i &= 1, 2, \ldots, n-1 \end{aligned} \tag{4.21}$$

Rewriting the above set of equations as

$$\alpha_{si+1} = f\alpha_{si} - g \qquad i = 1, 2, \ldots, n-1 \tag{4.22}$$

where

$$f = \frac{y_{eq}T_{so} - \rho z_0 T_{cm}}{y_{eq}T_{so}}, \;\; g = \frac{t}{y_{eq}T_{so}} \tag{4.23}$$

Here, $y_{eq}T_{so} > \rho z_0 T_{cm}$.
From the derivational similarity with $III - A$, we can solve for α_{s1} as (3.18). Hence, the minimum round time using n homogeneous intelligent sensor nodes, $T_{r,n}$ can be achieved as follows

$$\begin{aligned} T_{r,n} &= T_1 \\ &= t + \alpha_{s1} y_{eq} T_{so} = t + \frac{\frac{1}{\rho} + C_1'}{1 + C_2'} y_{eq} T_{so} \end{aligned} \tag{4.24}$$

Since the minimum round time on a single intelligent sensor node is

$$T_{r,1} = t + \frac{1}{\rho} y_{eq} T_{so} \tag{4.25}$$

the speedup is then

$$Speedup = \frac{T_{r,1}}{T_{r,n}} = \frac{t + \frac{1}{\rho} y_{eq} T_{so}}{t + \frac{\frac{1}{\rho} + C_1'}{1 + C_2'} y_{eq} T_{so}} \tag{4.26}$$

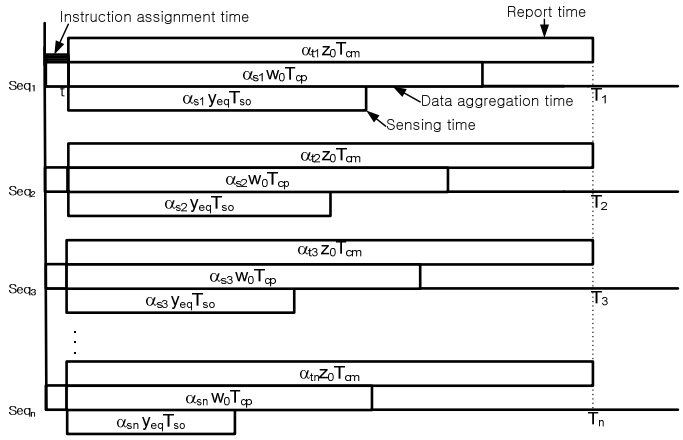

Figure 4.5: Timing diagram for multi channel flat wireless sensor network with homogeneous intelligent sensors with front-end processor.

4.4 Multi Channel with front-end processor

The timing diagram of the flat WSN with the n homogeneous intelligent sensor nodes is illustrated in Fig. 4.5. We assume here that $z_0T_{cm} > w_0T_{so}$, so that the speed data aggregation is faster than the speed of reporting. In other words, by intuitive sense, the data aggregation is needed to be ceased before or exactly when the reporting terminates. From the timing diagram (Fig. 4.5), one can set up the following corresponding recursive load distribution equations without considering the equivalent sensing speed, y_{eq}.

$$\alpha_{ti}z_0T_{cm} = \alpha_{ti+1}z_0T_{cm} \qquad i = 1, 2, \ldots, n-1 \tag{4.27}$$

From the intuitive similarity with subsection 3.4, we can solve for α_{t1} as $\frac{1}{n}$.
Hence, the minimum round time using n homogeneous intelligent sensor nodes, $T_{r,n}$ can be achieved as follows

$$T_{r,n} = T_1 = t + \frac{1}{n}z_0T_{cm} \tag{4.28}$$

Since the minimum round time on a single intelligent sensor node is

$$T_{r,1} = t + z_0T_{cm} \tag{4.29}$$

the speedup is then

$$Speedup = \frac{t + z_0T_{cm}}{t + \frac{1}{n}z_0T_{cm}} \tag{4.30}$$

Chapter 5

Performance evaluation

5.1 Feasible measurement instruction assignment time

Now we demonstrate the usage of the condition for the feasible measurement instruction assignment time constant by means of an illustrative example. We consider the scenario of SCnP with parameters, $n = 10$, $\rho = 1.0$, $T_{so} = 1.0$, $T_{cm} = 1.0$, and $T_{cp} = 1.0$. The speed parameters are set as $y = 1.0$, $z = 1.0$, $z_0 = 0.1$, and $w_0 = 0.1$. Based on the (3.24), η_i and γ_i for $i = 2, 3, \ldots, 10$ are given as TABLE 5.1. From the polarity of γ_i, $k = 4, 5, \ldots, 10$ and $l = 2, 3$. According to the condition (see (3.27)), the minimum value over the fourth and fifth rows of the TABLE 5.1 is given as 0.00099. Thus, the condition for the feasible measurement instruction assignment time constant is $0 \leq t < 0.00099$. For the check of feasibility of t, the sixth row of the TABLE 5.1 shows the optimal values of α_{si} for $i = 2, 3, \ldots, 10$ when $t = 0.0009$ sec, which is the feasible time value in the boundary. On the other hand, α_{s10} is given as a negative value which is obviously not a reasonable value for the α_s when $t = 0.001$ sec, which is an infeasible time value for the upper bound, 0.00099.

Index	2	3	4	5	6	7	8	9	10
η_i	0.25024	0.12512	0.06256	0.03128	0.01564	0.00782	0.00391	0.00195	0.00098
γ_i	1.50240	0.25122	−0.37439	−0.68719	−0.84360	−0.92180	−0.96090	−0.98045	−0.99022
η_k / γ_k	·	·	0.16710	0.04552	0.01854	0.00848	0.00407	0.00199	0.00099
$(1-\eta_l) / \gamma_l$	0.49902	3.48250	·	·	·	·	·	·	·
$\alpha_{si(\mathrm{opt})}$	0.25160	0.12535	0.06222	0.03066	0.01488	0.00699	0.00305	0.00107	0.00009
$\alpha_{si(\mathrm{inf\ eas})}$	0.25175	0.12537	0.06219	0.03059	0.01480	0.00690	0.00295	0.00098	−0.00001

Table 5.1: Example of the condition for the feasible measurement instruction assignment time.

t=0, Tso=1.0, Tcm=1.0, Tcp=1.0					
	ρ	z_0	w_0	z	y
vs. y	1.0 (SCnP,MCnP, SCP,MCP)	0.1 (SCnP,MCnP, SCP,MCP)	0.1 (SCnP,MCnP,MCP)	1.0 (SCnP,MCnP)	Variable
			0.2 (SCP)	0.1 (SCP)	
				2.0 (MCP)	
vs. z	1.0 (SCnP,MCnP, SCP,MCP)	0.1 (SCnP,MCnP, SCP,MCP)	0.1 (SCnP,MCnP, SCP,MCP)	Variable	1.0 (SCnP,MCnP)
					1.2 (SCP)
					0.1 (MCP)
vs. ρ	Variable	0.1 (SCnP,MCnP, SCP,MCP)	0.1 (SCnP,MCnP, SCP,MCP)	1.0 (SCnP,MCnP,SCP)	1.0 (SCnP,MCnP,MCP)
				2.0 (MCP)	1.2 (SCP)

Table 5.2: Simulation speed parameters.

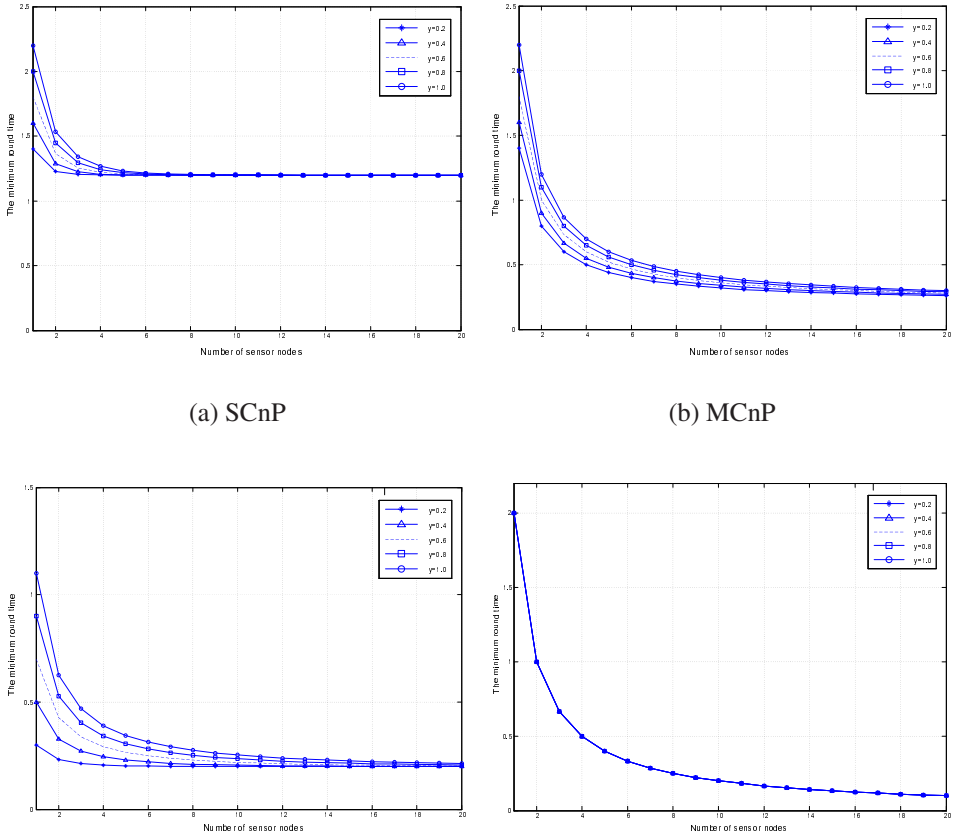

(a) SCnP (b) MCnP

(c) SCP (d) MCP

Figure 5.1: Total round time versus the number of senor nodes for the fully homogeneous cluster with variable y.

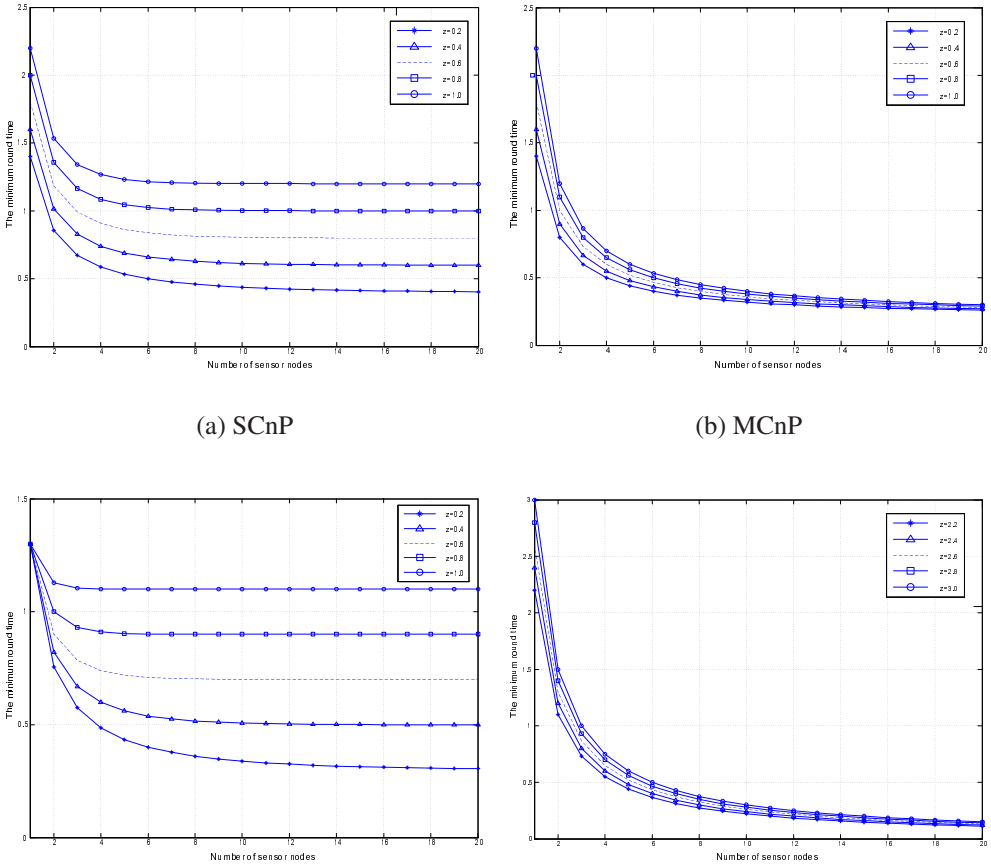

(a) SCnP

(b) MCnP

(c) SCP

(d) MCP

Figure 5.2: Total round time versus the number of sensor nodes for the fully homogeneous cluster with variable z.

5.2 Minimum round time

With common parameters $t = 0$, $T_{so} = 1.0$, $T_{cm} = 1.0$, and $T_{cp} = 1.0$, the minimum total round time of the four scenarios of SCnP, MCnP, SCP, and MCP are plotted against the number of sensor nodes in the fully homogeneous cluster for different sensing speeds, y, for different communication speeds, z, and for different information utility constants, ρ, using the speed parameters shown in the TABLE 5.2. Speed parameters for the scenarios of SCP and MCP are set according to the assumptions perviously mentioned for the minimum round time, $zT_{cm} < yT_{so}$, (3.55) and $zT_{cm} > yT_{so}$, (3.68) respectively. In Fig. 5.1, the five performance curves are obtained with $y = 0.2, 0.4, 0.6, 0.8$, and 1.0, respectively for the 4 scenarios. As shown in the subfigures, the longer the sensing delay, the longer the total round time, and the round time for the five cases saturates and converges to the value, $T_{r,\infty}$ which is independent of the sensing speed parameter, y as the number of sensor nodes increases. But the reduction is not too significant after just a few sensor nodes. Several similar intuitive curves have been shown in [20, 21]. Specifically, for the MCP scenario, the round time curves for 5 different values of sensing speed are exactly identical since round time is given as a function independent to the sensing speed parameter as shown (3.69). Similarly, in Fig. 5.2, the minimum total round time of the each scenario with $z = 0.2, 0.4, 0.6, 0.8$, and 1.0, is plotted respectively except MCP scenario with $z = 2.2, 2.4, 2.6, 2.8$, and 3.0. The subfigures show better total round time is obtained as the communication speed increases. The subfigures show better total round time is obtained as the communication speed increases. For all of the scenarios, the saturation of the total round time with respect to different values of z is shown as the number of sensor nodes increases. The convergence of the total round time for five different communication speeds is shown in Fig. 5.2(b) and Fig. 5.2(d) since $T_{r,\infty}$ is independent to the communication speed parameter, z ((3.47) and (3.72)).
In Fig. 5.3, the five performance curves are obtained with $\rho = 0.2, 0.4, 0.6, 0.8$, and 1.0, respectively for each scenario. In all subgraphs in Fig. 5.3, we can also see that the saturation of the total round time for five different information utility constants, ρ, as the number of sensor nodes increases. As we expect intuitively when the information utility gets higher (i.e., $\rho \to 1$), the total round time reduces. This is expected as the higher information utility constant decreases not only the sensing and reporting time at sensor nodes but also the data aggregation and reporting time at the clusterhead.

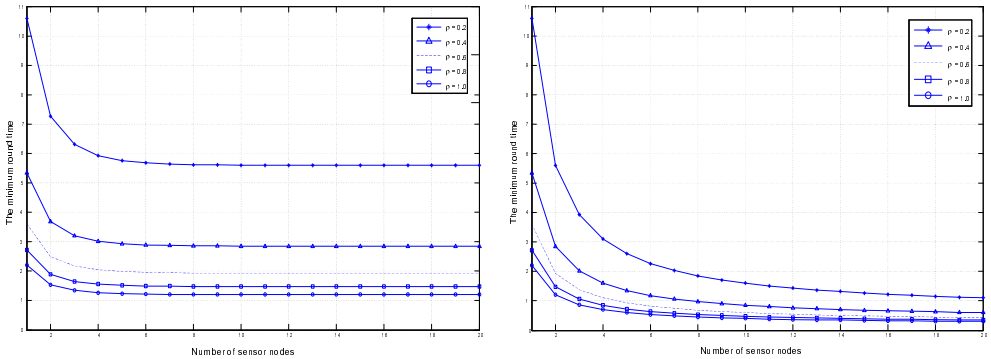

(a) SCnP (b) MCnP

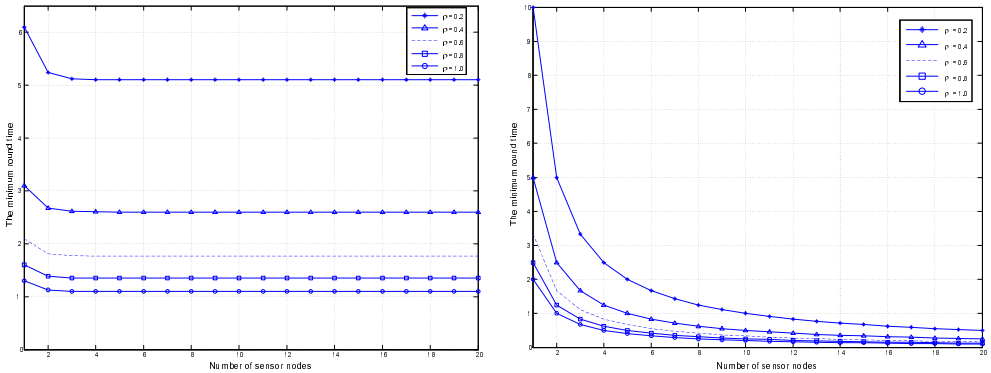

(c) SCP (d) MCP

Figure 5.3: Total round time versus the number of sensor nodes for the fully homogeneous cluster with variable ρ.

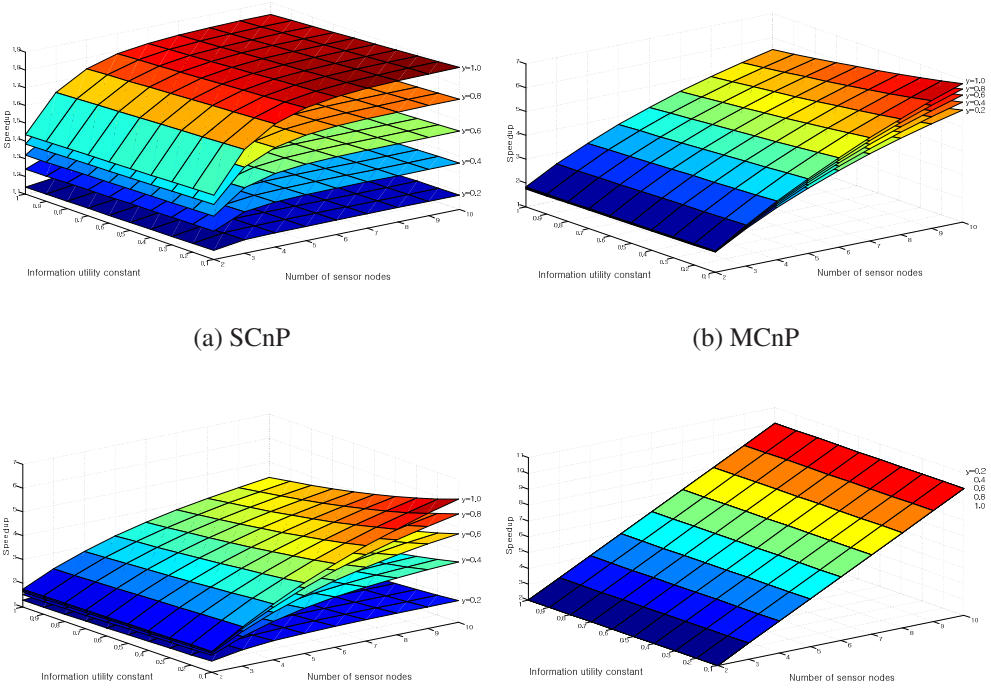

(a) SCnP (b) MCnP

(c) SCP (d) MCP

Figure 5.4: Speedup for the fully homogeneous cluster with variable ρ and y.

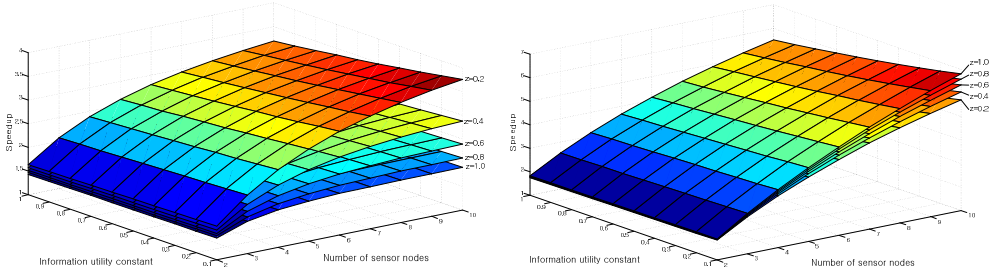

(a) SCnP

(b) MCnP

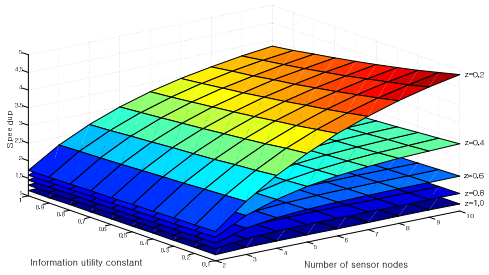

(c) SCP

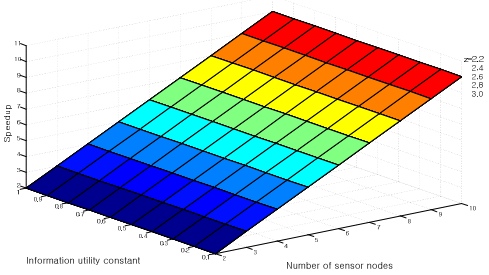

(d) MCP

Figure 5.5: Speedup for the fully homogeneous cluster with variable ρ and z.

5.3 Speedup

In Fig. 5.4 and 5.5, the speedup of the the 4 scenarios (SCnP, MCnP, SCP,and MCP) are described against the number of sensor nodes and the information utility constant in the fully homogeneous cluster for different sensing speeds, y and communication speeds, z, respectively. The same speed parameters used in previous subsection are applied. A better speedup characteristic can be seen as a result of the multiple channel comparing Fig. 5.4(a) to (b) (Fig. 5.5(a) to (b)) and Fig. 5.4(c) to (d) (Fig. 5.5(c) to (d)). It also can be seen that the front-end processors contribute to the better speedup comparing Fig. 5.4(a) to (c) (Fig. 5.5(a) to (c)) and Fig. 5.4(b) to (d) (Fig. 5.5(b) to (d)). All of the plots except for the MCP scenario show the speedup saturation as the number of sensor nodes increases. Especially, Fig. 5.4(d) and Fig. 5.5(d) show speedup given as a linearly increasing curve of first order n. As we previously mentioned, in the case that the instruction assignment time, t is negligible, speedup is achieved as a scalable function by n, which is independent of the speed parameter y and z (see (3.71)). As a reminder, the value of speedup saturation of the 4 scenarios are given as (3.29), (3.48), (3.62), and (3.72). Interestingly, a smaller increment in the speedup according to the variation of the information utility is shown relative to the case of the variation of the number of sensor nodes. The smaller sensitivity of the information utility constant in the speedup can be mathematically analyzed in that the information utility constant, ρ appearing in both numerator and denominator seems to largely cancel out. A modestly better speedup characteristic as information utility decreases implies that relatively more performance enhancement in round time can be achieved by additional sensor nodes when the accuracy of collected data is low.

5.4 Energy Dissipation

Power usage in wireless sensor nodes has been studied for finite amounts of non renewable energy in sensor networks. A radio model has been developed to model the energy dissipated by a sensor node when transmitting and receiving data [25]. To transmit a k bit data a distance d, the energy dissipated is

$$E_{tx}(k,d) = E_{elec} \cdot k + \varepsilon_{amp} \cdot k \cdot d^2 \tag{5.1}$$

and to receive the k bit data, the radio expends

$$E_{rx}(k) = E_{elec} \cdot k \tag{5.2}$$

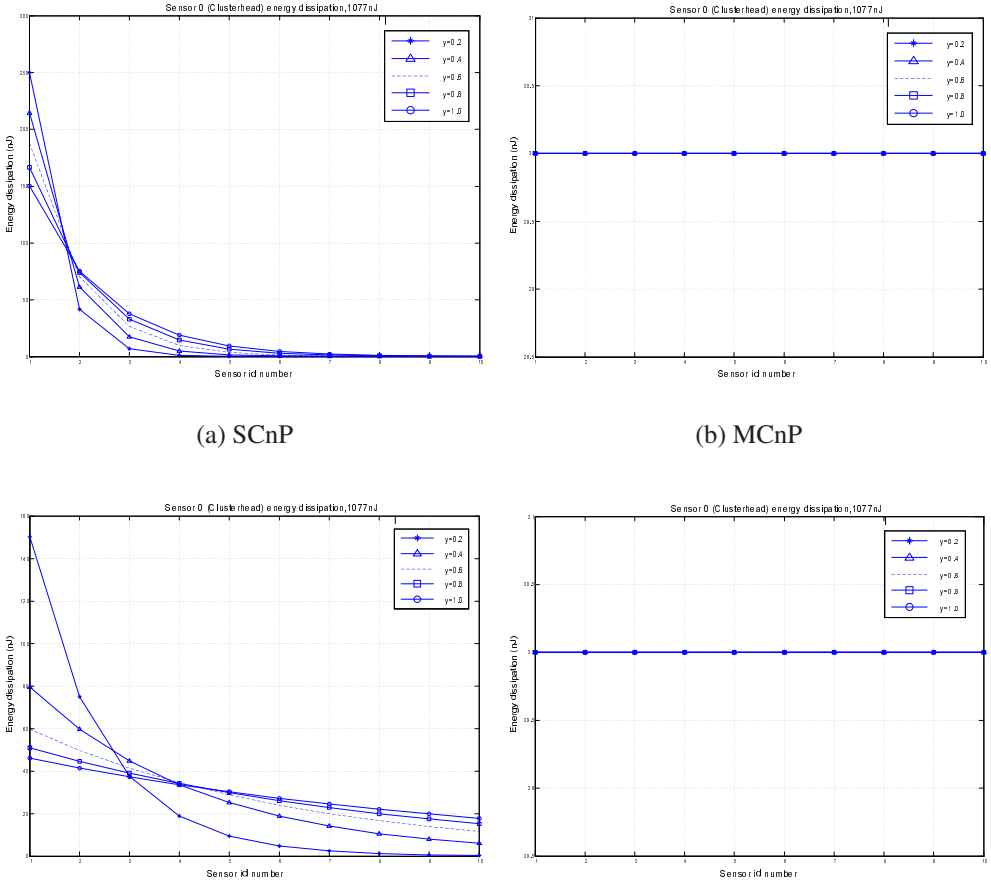

(a) SCnP (b) MCnP

(c) SCP (d) MCP

Figure 5.6: Energy dissipation versus sensor id number for the fully homogeneous cluster with variable y.

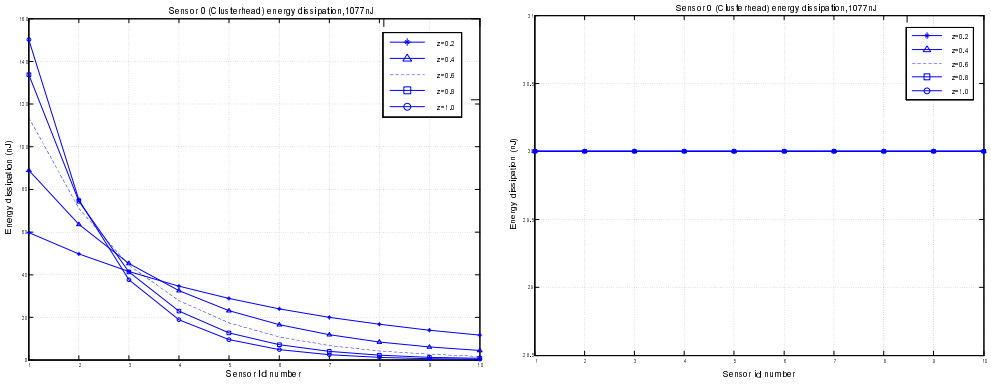

(a) SCnP

(b) MCnP

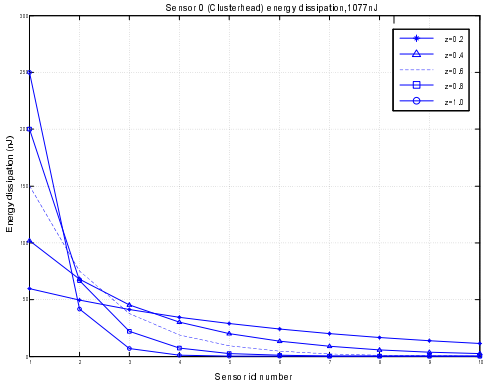

(c) SCP

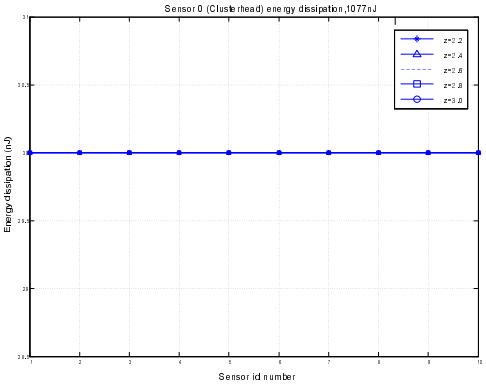

(d) MCP

Figure 5.7: Energy dissipation versus sensor id number for the fully homogeneous cluster with variable z.

Here, the parameter, k can be substituted with the normalized fraction of data, αs, computed by DLT. The DLT based analysis of the wireless sensor energy dissipation has been studied using the first order radio model [20]. For this work, we assume that the radio model also follows the first order radio model. Also, we consider an energy dissipation other than the radio, mainly in the processors in the sensor nodes. It is well known that the radio energy dissipation overwhelms the other losses such as processing energy dissipation. However, energy dissipation in processing and data aggregation at the clusterhead seems important to be considered in the meaning of DLT since clusterhead deals with relatively large amount of collected data from each sensor node.

The following notation and the corresponding value are used for our simulation.

d : distance from each sensor node to clusterhead $50m$. (distance from clusterhead to sink, $100m$).

E_{elec} : 50 nJ/b.

ε_{amp} : 100 $pJ/b/m^2$. For the analysis of the processing energy dissipation, we use the experimental parameters used in [26]. From [26] a Mica2 sensor mote is specified as a 38.4$Kbps$ radio that operates at $3V$ (2xAA Batteries), or $27nJ/b$ $(27W \cdot s/b)$ processing cost.

Based on the first order radio model and the computed processing energy dissipation by using Mica2 specifications, the total energy dissipation of the 4 scenarios (SCnP, MCnP, SCP, and MCP) are plotted in Fig. 5.6 against 10 sensors including the clusterhead in the homogeneous cluster for different sensing speeds, y, with the same values of the parameters used in the previous simulation for the total round time for different sensing speeds. As shown in Fig. 5.6(a) and 5.6(c), the energy dissipation at each sensor node unevenly decreases as the sensor node number increase. It is because the energy dissipation is mainly related to the amount of collected and reported data. As the sensing speed is faster, the first few sensor nodes would have more data to be processed so that more energy dissipation is highly concentrated on the first few sensor nodes as shown in Fig. 5.6(a) and 5.6(c). The energy dissipation at a clusterhead is computed as an identical amount, $1077nJ$ for the four scenarios. This is expected as the clusterhead processes all the reported data which depends on only the information utility constant and reports the perfectly aggregated data (unit amount) to a sink. Specially, for the MCnP and MCP scenario, the energy dissipation curves for 5 different values of sensing speed are exactly identical to a constant value since the total data is equally distributed to each sensor node due to the simultaneous sensing and reporting enabled by muti-channels under the fully homogeneous cluster case as shown (3.43).

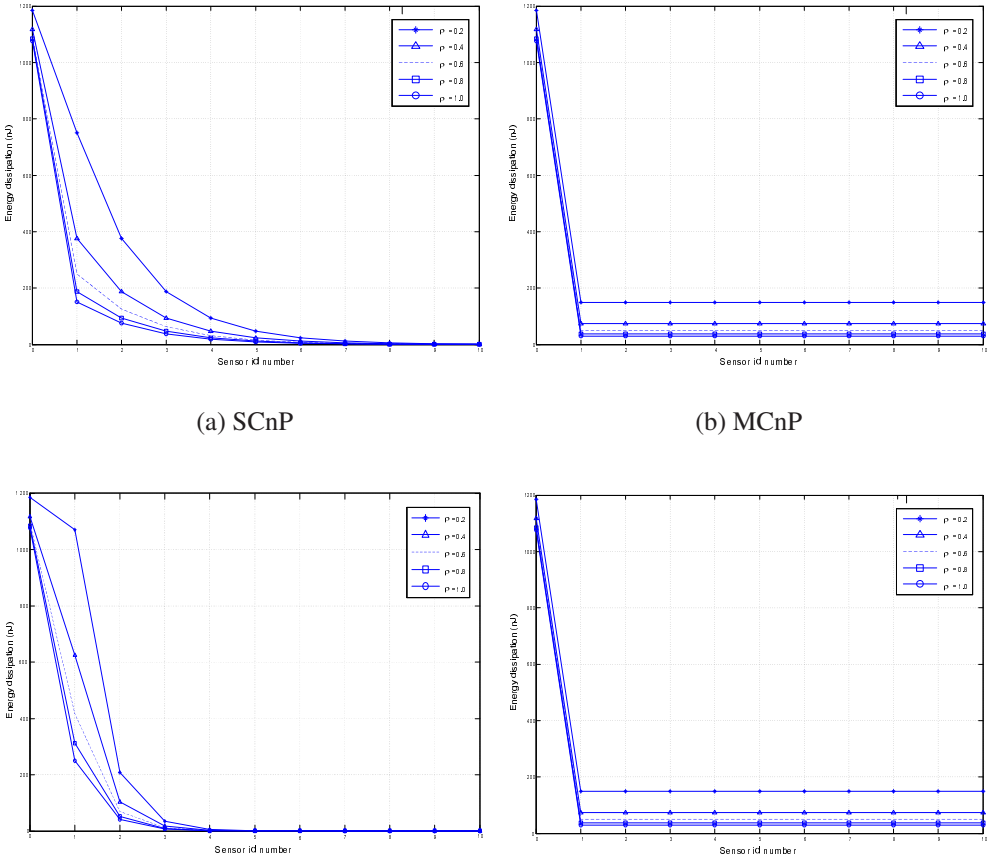

(a) SCnP

(b) MCnP

(c) SCP

(d) MCP

Figure 5.8: Energy dissipation versus sensor id number for the fully homogeneous cluster with variable ρ.

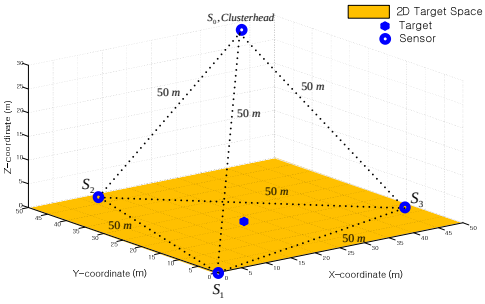

(a) 3D Cluster model with varying target location.

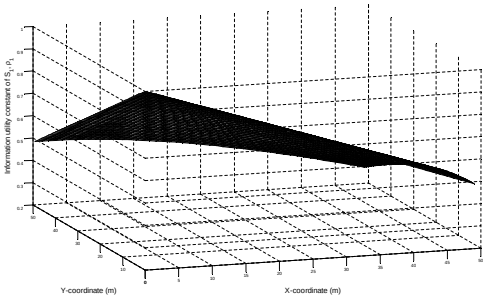

(b) Information utility constant, ρ_1 vs Target location

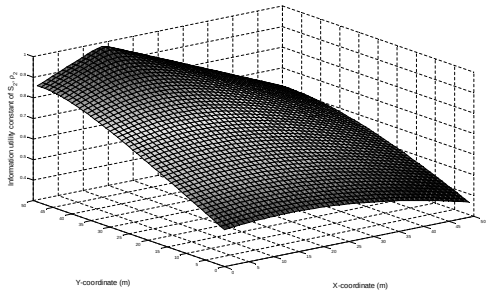

(c) Information utility constant, ρ_2 vs Target location

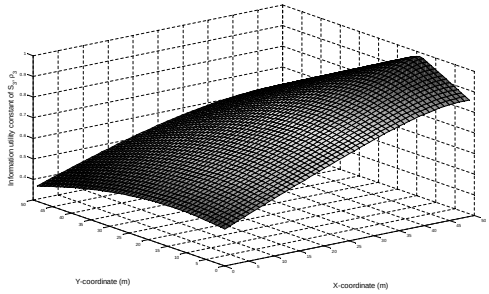

(d) Information utility constant, ρ_3 vs Target location

Similarly, in Fig. 5.7, the total energy dissipation of the 4 scenarios is plotted against the number of sensor nodes in the homogeneous cluster for different communication speeds, z, with the values of the parameters used in the previous simulation for the total round time for different z. The plots show intuitively similar results with the result in the case of different sensing speed. In Fig. 5.8, the total energy dissipation of the 4 scenarios are plotted against the number of sensor nodes in the homogeneous cluster for different information utility constant, ρ with the values of the parameters used in the previous simulation for the total round time for different ρ. Here, sensor number 0 denotes the clusterhead. Intuitively, the smaller the information utility constant (that is more redundant data), the more energy dissipation as shown in Fig. 5.8. As we mentioned before, the clusterhead processes all the reported data which depends on the information util-

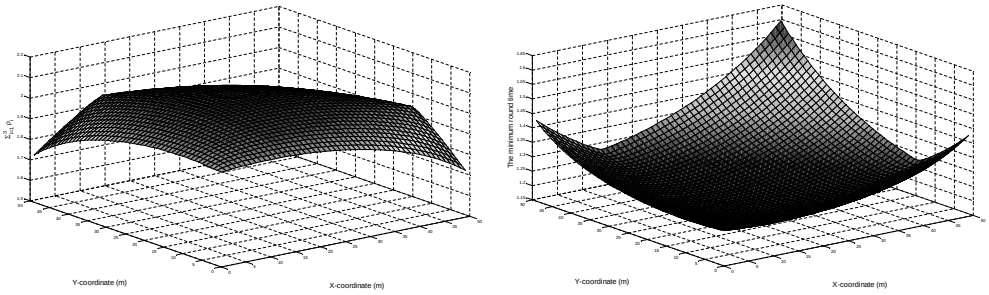

(e) Total information utility constant vs Target location

(f) Minimum round time vs Target location.

Figure 5.9: MCnP scheduling for 3D Cluster model

ity constant so that the energy dissipation at the clusterhead varies according to the information utility constant.

5.5 3D Cluster Model

Simulation is carried out to illustrate the relationship between different information utility constants according to the variation of a target location model involving the minimum round time. We consider a three dimensional tetrahedron cluster with $50m$ edges, three sensor nodes (S_1,S_2, and S_3) positioned on the vertices of a base triangle and a clusterhead (S_0) positioned on the other vertice as illustrated in Fig. 5.9(a). The three sensor nodes could be ground based sensing stations and the clusterhead is airborne. The target location can be varied on the 2D square target space as shown in Fig. 5.9(a). In this simulation, we use the estimation technique introduce in [6] so that each sensor node has a value of information utility constant, 0.7, especially when the target lies at the center of the base triangle. That is the heterogeneous information utility constants are generated as the target location varies. Here, the multi channel with no front end processor (MCnP) scheduling scenario is applied for the simulation with the same values of the speed parameters used in the previous simulation for the total round time for different ρ. The information utility constant is illustrated when the target is moving in the square 2D target space as shown in Fig. 5.9(b), 5.9(c), and 5.9(d). As we expect, the figures show a convex peak at the location of the each sensor. In other words, the

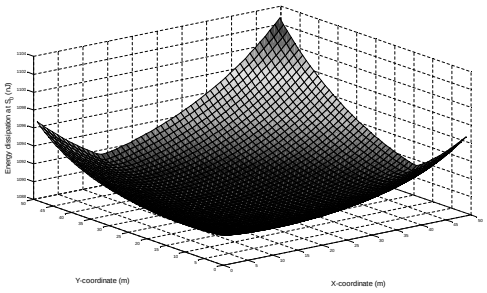

(a) Energy dissipation at S_0(clusterhead) vs Target location.

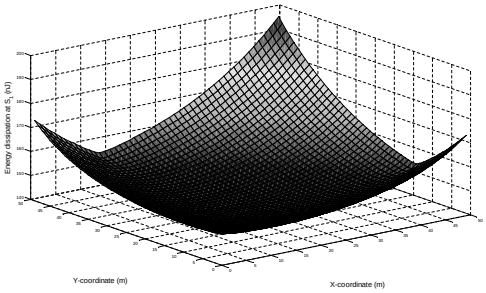

(b) Energy dissipation at S_1 vs Target location.

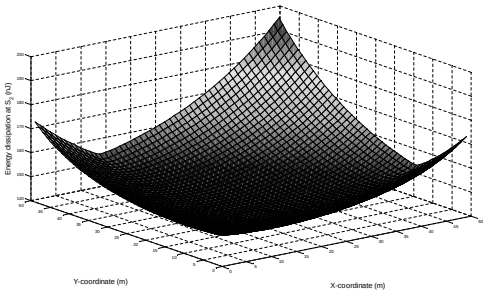

(c) Energy dissipation at S_2 vs Target location.

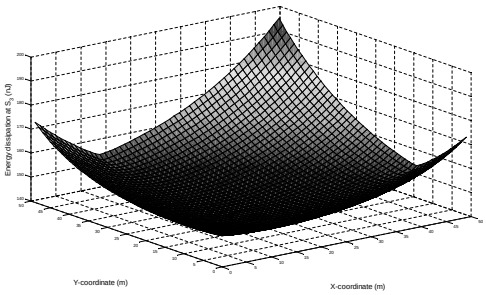

(d) Energy dissipation at S_3 vs Target location.

Figure 5.10: Energy dissipation versus Target location MCnP scheduling.

corresponding information utility constant increases as the target moves toward each of the sensor nodes as expected.
As we derived in (3.42), the minimum round time for MCnP scheduling scenario inversely depends on the value of the summation of the information utility constants of each sensor node. Fig. 5.9(e) shows the convex distribution of the value of $\sum_{i=1}^{3} \rho_i$ over the region of the target space. As we expect, a concave result for the minimum round time is shown in Fig. 5.9(f) as a vertical flipped version of Fig. 5.9(e).
Fig. 5.10 shows the energy dissipation of each sensor (S_0, S_1, S_2, and S_3) over the region of the target space. From Fig. 5.10 we can recognize all plots are depicted as a similar shape by each other with Fig. 5.9(f). This is because the amount of reported data from each sensor node and total amount of the collected data at clusterhead also inversely depends on the sum of the information utility constants of each sensor node (see (3.41)). Similarly, in MCnP scenario, we can also expect identical result for the energy dissipation at the sensor nodes, S_1, S_2, and S_3 as shown in Fig. 5.9.

Chapter 6

Conclusion and Open Questions

In this paper, closed form solutions for the minimum round time for several scenarios of single cluster wireless sensor networks are derived. The performance of these scenarios are examined according to different sensing speeds, communication speeds, and information utility constants. The condition for feasible measurement instruction assignment time is derived and a numerical example is presented to describe the importance of DLT feasibility by demonstrating the operation of the condition. The special bounds for the ratio of speed parameters for the maintenance of the minimum round time are also derived. By using an equivalent speed parameter, it is shown that a multi-cluster based WSN can be analyzed as a flat wireless sensor network without clusters. The performance of clustered WSN networks is shown by using a deterministic analysis method, divisible load theory. By direct deterministic approaches, our work gives a general idea of the performance of WSN.

For extensions to our work, the analysis of a multi-cluster WSN topology would be interesting. A more comprehensive study concerning the relationship between the speed parameters and the information utility constant and the corresponding performance including speedup and asymptotic performance is worth addressing for future work. As for the more rigorous analytic results, the study of the following issues are also expected to extend our study:

• The analytical model for a WSN with direct communication between sensor nodes (Ad hoc WSN).

• The analysis of performance variation according to the quality of data aggregation.

• The effect of the heterogeneous speed parameters including the information utility.

• The analysis of special bounds for the related parameters (i.e., speed parameters, instruction assignment time, and information utility) under a heterogenous WSN.

Bibliography

[1] Akyildi, I. F., Su, W., Sankarasubramaniam, Y., and Cayirci, E.
Wireless sensor networks: a survey, Computer Networks
The International Journal of Computer and Telecommunications Networking, **38** (2002), 393-422.

[2] Haas, Z., and Tabrizi, S.
On Some Challenges and Design Choices in Ad-Hoc Communications
IEEE MILCOM, (1998).

[3] Heinzelman, W. B., Chandrakasan, A. P., and Balakrishnan, H.
An application - specific protocol architecture for wireless microsensor networks
IEEE Transactions on Wireless Networking, (2002).

[4] Lindsey, S., and Raghavendra, C.
PEGASIS: Power-efficient gathering in sensor information systems
Proceedings of IEEE Aerospace Conference, **3** (2002), 1125-1130.

[5] Hightower, J., and Borriello, G.
Location systems for ubiquitous computing
IEEE Computer on Communications, (2001), 57-66.

[6] Li, H., Jiang, S., and Wei, G.
Information-Accuracy-Aware Jointly Sensing Nodes Selection in Wireless Sensor Networks
Mobile Sensor Network Conference, (2006), 736-747.

[7] Bharadwaj, V., Ghose, D., Mani, V., and Robertazzi, T. G.
Scheduling Divisible Loads in Parallel and Distributed Systems
IEEE Computer Society Press, (1996)

[8] Bharadwaj, V., Ghose, D., and Robertazzi, T. G.
Divisible Load Theory: A New Paradigm for Load Scheduling
in Distributed Systems
Cluster Computing, **6** (2003), 7-18.

[9] Robertazzi, T. G.
Ten Reasons to Use Divisible Load Theory
Computer, **36** (2003), 63-68.

[10]Cheng, Y. C., and Robertazzi, T. G.
Distributed Computation with Communication Delays
IEEE Transactions on Aerospace and Electronic Systems
24 (1988), 700-712.

[11]Cheng, Y. C., and Robertazzi, T. G.
Distributed Computation for a Tree Network with
Communication Delays
IEEE Transactions on Aerospace and
Electronic Systems, **26** (1990), 511-516.

[12]Bataineh, S., and Robertazzi, T. G.
Bus-Oriented Load Sharing for a Network of Sensor Driven Processors
IEEE Transactions on Systems, Man, and Cybernetics, **21** (1991).

[13]Kim, H. J., Jee, G. I., and Lee, J. G.
Optimal Load Distribution for Tree Network Processors
IEEE Transactions on Aerospace and Electronic Systems, **32**
(1996), 607-612.

[14]Sohn, J., and Robertazzi, T. G.
Optimal Divisible Job Load Sharing on Bus Networks
IEEE Transactions on Aerospace and Electronic Systems, **32**
(1996), 34-40.

[15]Sohn, J., and Robertazzi, T. G.
Optimal time-varying load sharing for divisible loads
IEEE Transactions on Aerospace and Electronic Systems, **34** (1998)
907-923.

[16]Ko, K., and Robertazzi, T. G.

Scheduling in an Environment of Multiple Job Submissions
Proceedings of the 2002 Conference on Information Sciences and Systems, (2002).

[17]Bharadwaj, V., Ghose, D., and Mani, V.
Optimal Sequencing and Arrangement in Distributed Single-Level Networks with Communication Delays
IEEE Transactions on Parallel and Distributed Systems, **5** (1994), 968-976.

[18]Lin, X., Ying, L., Deogun, J., and Goddard, S
Real-Time Divisible Load Scheduling for Cluster Computing
Technical report TR-UNL-CSE-2006-0016
University of Nebraska-Lincoln, (2006).

[19]Bharadwaj, V., Ghose, D., and Mani, V.
A Study of Optimality Conditions for Load Distribution in Tree Networks with Communication Delays
Technical Report 423/GC/02-92
Indian Institute of Science, (1992).

[20]Moges, M., and Robertazzi, T. G.
Wireless Sensor Networks: Scheduling for Measurement and Data Reporting
IEEE Transactions on Aerospace and Electronic Systems, **42** (2006), 327-340

[21]Gamboa, C. F., and Robertazzi, T. G.
Efficient Scheduling for Sensing and Data Reporting in Wireless Sensor Networks
2006 Conference on Information Sciences and Systems, (2006)

[22]Hung, J. T., and Robertazzi, T. G.
Scalable Scheduling for Clusters and Grids using Cut Through Switching
International Journal of Computers and their Applications, **26** (2004), 147-156

[23]Hung, J. T., and Robertazzi, T. G.
Divisible Load Cut Through Switching in Sequential Tree Networks
IEEE Transactions on Aerospace and Electronic Systems, **40** (2004), 968-982.

[24]Bataineh, S., Hsiung, T., and Robertazzi, T. G.
Closed Form Solutions for Bus and Tree Networks of Processors
Load Sharing a Divisible Job
IEEE Transactions on Computers, **43** (1994), 1184-1196.

[25]Heinzelman, W., Chandrakasan, A., and Balakrishnan, H.
Energy-Efficient Communication Protocol for Wireless Microsensor Networks
Proceedings of the 33rd Annual Hawaii International
Conference on System Sciences, (2000), 3005-3014.

[26]Younis, O., and Fahmy. S.
An experimental study of routing and data aggregation in sensor networks
Proceedings of the IEEE International Workshop on Localized
Communication and Topology Protocols for Ad Hoc Networks, (2005).